

Ernst-Reuter-Platz 1  
Gebäude BH-N, Raum 802  
10587 Berlin

April 28, 2020

To the Editor Roberto Greco,

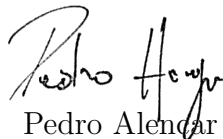
On behalf of all authors, I would like to thank the Editor and the Referees for taking their valuable time to make our work better. We fully agree with your recommendations.

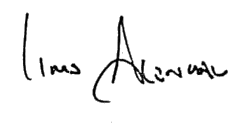
We performed a complete review of the text, including change of order and structure of paragraphs and subsections. We believe that now the text is much clearer and less ambiguous. We found, after the review, that many paragraphs had disjoint information and, sometimes, the information was rather scattered between two paragraphs. We hope to have fixed this flaw.

A native speaker and professional proofreader made full revision of the text regarding grammar, structure and style, to make the language clearer. Besides, the supplement material was reformulated with the addition of more information.

We hope that this new version meets the requirements and expectations of the Hydrology and Earth System Science Journal.

Sincerely,

  
Pedro Alencar



# Physically-based model for gully simulation: application to the Brazilian Semiarid Region

Pedro Henrique Lima Alencar<sup>1,2</sup>, José Carlos de Araújo<sup>2</sup>, and Adunias dos Santos Teixeira<sup>2</sup>

<sup>1</sup>TU Berlin, Institut für Ökologie, 10587 Berlin, Germany

<sup>2</sup>Federal University of Ceará, Departamento de Engenharia Agrícola, Fortaleza, Brazil

**Correspondence:** Pedro Alencar (pedro.alencar@campus.tu-berlin.de); José Carlos de Araújo (jcaraujo@ufc.br)

**Abstract.** Gullies are one of the most relevant erosion processes, connected to land degradation and desertification, in special in arid and semiarid regions. Despite its role, gully erosion is neglected by many models and researches. This study presents a physically-based model for small permanent gullies, typical in the Brazilian Semiarid Region. The model consists of coupling two previous models, those by Foster and Lane (1983) and Sidorchuk (1999). As both models require input data of peak discharge and duration, different rain intensities were tested. The rain intensity that suited gully erosion modelling best was the 30-minute intensity. The Foster and Lane model supplied a better response for smaller areas, where bed-channel erosion is more pronounced. The Sidorchuk model presented a better performance in larger sections, where wall erosion becomes more prominent. The experimental area is located in the semiarid State of Ceará, Brazil, in which the land use is characterised by agriculture and livestock. We measured and modelled three gullies ageing almost six decades. The threshold between the prevailing domains of each process (channel bed or wall erosion) is based on the cross-section area; and it is intrinsically connected to wall erosion: for the case study, the threshold area was approximately 2 m<sup>2</sup>. The final model, hereby called FL-SM (Foster & Lane and Sidorchuk Model) performed very well, with Nash-Sutcliffe coefficient of 0.846.

*Copyright statement.*

## 1 Introduction

On our way to sustainable development and environmental conservation, soil erosion by water was pointed out as a key problem to be faced in the 21<sup>st</sup> century (Borrelli et al., 2017; Poesen, 2018). The impact of water-driven soil erosion, on economy and food supply alone, represents an annual loss of US\$ 8 to 40 billion; a reduction in food production of 33.7 million tonnes; an increase in water consumption by 48 km<sup>3</sup>. These effects are felt more severely in countries like Brazil, China and India; and in low-income households worldwide (Pimentel et al., 1995; Nkonya et al., 2016; Sartori et al., 2019). Estimations on total investments to mitigate land-degradation effects on site (e.g. productivity losses) and their off-site effects (e.g. biodiversity losses, water body siltation) lead to more alarming values, averaging US\$ 400 billion yr<sup>-1</sup> (Pimentel et al., 1995; Nkonya et al., 2016). Nonetheless, those values were obtained by estimations of soil erosion using USLE (Universal Soil Loss Equation) or

similar methods, none considering gully erosion, thus the real economical and social impacts of soil erosion are not completely comprehended.

25 Notwithstanding, soil degradation had already been a national issue in the first years of the 20<sup>th</sup> century in the USA, for instance, being reported by the USDA and the National Conservation Congress, with over 44 thousand km<sup>2</sup> of abandoned land due to intense erosion. By the end of the 1930's this number had increased to over two hundred thousand km<sup>2</sup> (Montgomery, 2007). Among soil erosion mechanisms, gully erosion plays a relevant role in sedimentological processes in watersheds, since it frequently is the major source of sediment displacement (Vanmaercke et al., 2016). Ireland et al. (1939) observed early the  
30 effect of intense land-use change on gully formation, mainly due to alteration on land-cover and flow path direction. These landscape modifications were connected to runoff acceleration and/or concentration, therefore, triggering gullies.

Gully erosion consists of a process that erodes one (or a system of) channel(s) that starts due to the concentration of surface water discharge erosion during intense rainfall events (Bernard et al., 2010). The concentrated flow causes a deep topsoil incision and may reach the groundwater table (Starkel, 2011). Gullies are connected to anthropogenic landscape modifications  
35 and to land use and land cover changes, as observed in the Cerrado biome in Brazil (Hunke et al., 2015). On the other hand, the presence of vegetation may prevent soil erodibility both by increasing cohesion forces and enhancing soil structure (Li et al., 2017; Vannoppen et al., 2017). Maetens et al. (2012) suggested that land-use changes lead to runoff changes and, hence, directly affect erosive processes. Gully erosion can also be affected by climate change, e.g., an increase of rainfall intensity could lead to higher erosive potential (Nearing et al., 2004; Montenegro and Ragab, 2012; Figueiredo et al., 2016; Panagos  
40 et al., 2017).

Gullies also play a relevant role in the connectivity of catchments (Verstraeten et al., 2006; Molina et al., 2009), allowing more sediment to reach water bodies and, thus, increasing siltation (de Araújo et al., 2006). Gullies are also strongly dependent of landscape factors. With the advance of machine-learning techniques and the use of large data sets, some of the factors that mostly influence gully formation were identified, such as lithology, land use and slope. Some indexes were also pointed as  
45 relevant to indicate gully initiation, as the Normalized Difference Vegetation Index, Topography Wetness Index and Stream Power Index (Arabameri et al., 2018, 2019; Azareh et al., 2019).

For being particularly relevant among the erosion processes, gullies execute a great pressure on landscape development: they change the water-table height, alter sediment dynamics and increase runoff (Valentin et al., 2005; Poesen, 2018; Yibeltal et al., 2019). They represent an increasing risk to society and environment for affecting land productivity, water supply, floods,  
50 debris flow and landslides (Liu et al., 2012, 2016; Ruljgaljig et al., 2017; Wei et al., 2018). Gullies also have a large impact on economy due to high mitigation costs, a reduction of arable fields, a decrease of groundwater storage, an increase of water and sediment connectivity and more intense reservoir siltation (Verstraeten et al., 2006; Pinheiro et al., 2016). The assessment of gully impacts on production costs in an arid region of Israel showed that costs of gully mitigation represent over 5% of total investments, and production losses are as large as 37 % (Valentin et al., 2005).

55 Despite their relevance to hydro-sedimentological processes, gullies are often neglected in models (De Vente et al., 2013; Poesen, 2018), and should be directly addressed (Paton et al., 2019). However, gully erosion is a process with the interaction of many variables, many of them difficult to assess (Bernard et al., 2010; Castillo and Gómez, 2016): according to Bennett

and Wells (2019), for instance, no model has ever been presented to clearly explain the process of gully formation. Among the models that do consider gully erosion, the use of empirical approach prevails (Thompson, 1964; Watson and Laflen, 1986; Woodward, 1999; Nachtergaele et al., 2001, 2002; Poesen et al., 2002; Yao et al., 2008; Wells et al., 2013); whereas others focus primarily on physically-based algorithms (Foster and Lane, 1983; Storm et al., 1990; Hairsine and Rose, 1992; Ascough et al., 1997; Sidorchuk, 1999; Alonso et al., 2002; Sander et al., 2007; Dabney et al., 2015).

It is, therefore, an important milestone to understand how gully erosion starts and develops (Poesen, 2018). The objective of this work is to propose a physically-based model that predicts growing dynamics and sediment production in small permanent gullies in a hillslope scale. Most of the basins around the world do not have subdaily rainfall data for obtaining the discharge characteristics for storm events that cause gully erosion (de Araújo, 2007). As registered in literature by many authors (Ireland et al., 1939; Katz et al., 2014), road construction is a main driver for gully initiation. It was assumed that small permanent gullies are the result of active erosive processes that form channels by concentrated flow and do not interact with groundwater. Normally, these gullies could be remediated by regular tillage process, but in abandoned or unclaimed land they usually remain untreated for long periods.

## 2 MATERIALS AND METHODS

### 2.1 Study area

The Brazilian Semiarid Region (1 million km<sup>2</sup>) is covered mainly by the Caatinga biome with predominantly bushes and broadleaf deciduous vegetation. (de Araújo and Piedra, 2009; Pinheiro et al., 2013). The region is prone to droughts and highly vulnerable to water scarcity (Coelho et al., 2017). More than 25 million people live in this region, where agriculture (maize, beans, cotton) and livestock are of utmost socio-economic relevance. Usually, rural communities use deleterious practices, such as harrowing and field burning, which enhance the risk of intense erosive processes. These characteristics lead to a scenario of soil erosion and water scarcity with high social, economic and environmental consequences (Sena et al., 2014). Erosion in general (and gullies in particular) increases local hydric vulnerability due to reservoir siltation (de Araújo et al., 2006) and water-quality depletion (Coelho et al., 2017).

The study area is located in the Madalena Representative Basin (MRB, 75 km<sup>2</sup>, state of Ceará, north-eastern Brazil; see Figure 1), inserted in the Caatinga biome, a dry environment with a semiarid hot BSh climate, according to the Köppen classification (Gaiser et al., 2003). The annual precipitation averages 600 mm, concentrated between January and June (Figure 2); and the potential evapotranspiration totals 2,500 mm.yr<sup>-1</sup>. Geologically, the basin is located on top of a crystalline bedrock with shallow soils and a limited water storage capacity. The rivers are intermittent and runoff is low, typically ranging from 40 to 60 mm.yr<sup>-1</sup>. The basin is located within a land reform settlement with 20 inhabitants per km<sup>2</sup>, whose main economic activities are agriculture (specially Zea mays), livestock and fishing (Coelho et al., 2017; Zhang et al., 2018).

Three gullies were selected for this study, all located on the eastern portion of the basin. The studied gullies have the following dimensions (average  $\pm$  standard deviation): projection area (317 $\pm$ 165 m<sup>2</sup>), length (38  $\pm$  6 m), volume (42  $\pm$  25 m<sup>3</sup>), depth (0.44  $\pm$  0.25 m) and eroded mass (61  $\pm$  36 Mg). Despite their small sizes, they possess a significant impact on

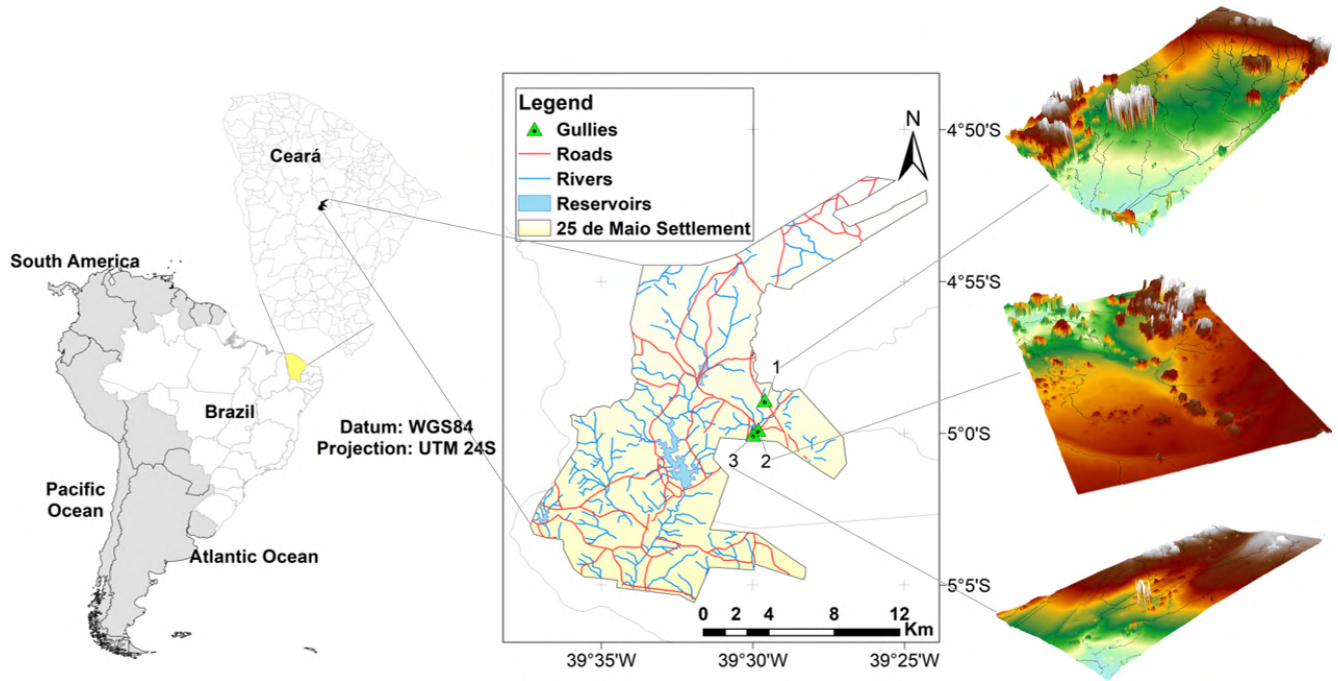


**Figure 1.** Location of the study area and the gully sites (gullies 1, 2 and 3) and the digital elevation models. The roads, rivers and reservoirs were mapped by Silva et al. (2015).

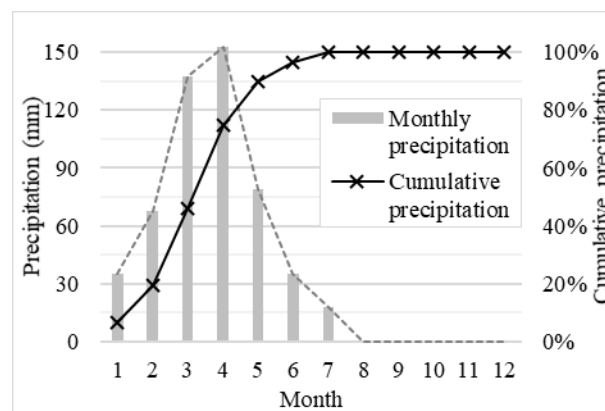


**Figure 2.** Monthly precipitation (median) and cumulative precipitation at MRB from 1958 to 2015.

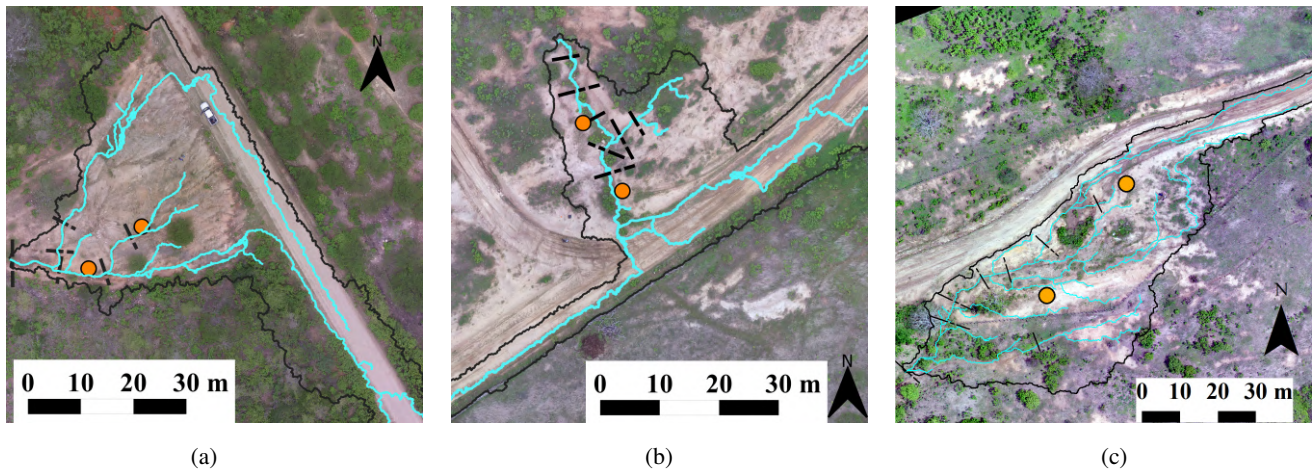


**Figure 3.** Aerial photogrammetry of the studied gullies. Note that they are at the margin of the road, receiving the concentrated flow diverged from it. The continuous black line represents the catchment boundaries; the blue line represents the flow paths; the dashed black lines are the cross-sections used on the validation of the model and; the orange dots are the soil sampling points - (a) gully 1; (b) gully 2; (c) gully 3.

the landscape for reducing productive areas and soil fertility. According to the information obtained from local villagers, gully erosion started immediately after the construction of a country road in 1958 (Figure 3). Before the construction, the sites were covered by Caatinga vegetation (Pineiro et al., 2013). The road modified the natural drainage system and does not provide for any side nor outlet ditches, therefore generating a concentrated runoff at its side. This has caused excessive runoff on the hillslopes and triggered gully erosion.

## 2.2 Topography survey

The assessment of the gully data was achieved using an Unmanned Aerial Vehicle (UAV), a technique applied in other regions as well (Vinci et al., 2015; Wang et al., 2016; Pineux et al., 2017; Gudino-Elizondo et al., 2018). A UAV equipped with a 16 MP camera (4000 x 4000 pixels) and a view field of 94 % was used. The flight was at 50 m altitude with a frontal overlap of 80 % and lateral overlap of 60 %. For the geo-referencing of the mosaic, five ground control points were deployed, which were evenly distributed in each area, both in high and low ground. The coordinates were collected using a stationary GNSS – RTK (L1/L2) system with centimetre-level accuracy. The Digital Surface Model was produced using the Structure from Motion technique. The process consists of a three-dimensional reconstruction of the surface, derived from images and the generation of a dense cloud of 3D points based on the matching pixels of different pictures and Ground Control Points (GPCs); the processing result is a model as accurate as one obtained by laser surveys (e.g., Light detection and ranging - LiDAR), but cheaper and less time consuming (Castillo et al., 2015; Agüera-Vega et al., 2017; Gudino-Elizondo et al., 2018). From the Digital Surface Model, the Digital Elevation Model (DEM) was derived. The ground sample distance (pixel size) obtained is of four to five centimetres and the digital models have high precision, with a vertical position error of around one centimetre and horizontal error of six



millimetres. The vegetation, yet sparse, was an obstacle to increasing the quality of the survey. However, as the focus of this study was the gully cross-section geometry, vegetation interference was acceptably low.

### 2.3 Soil data

At the gully sites, soil surveys were carried out to assess the properties and parameters required to implement the model: undisturbed soil samples were collected (see Figure 3) at depths of 0.10 m, 0.30 m and 0.50 m. At the depth of 0.50 m, a well-defined horizon C, rich in rocks and soil under formation, was identified. The maximum depth of the non-erodible layer ranged from 60 to 75 cm in all gullies. We performed grain-size distribution, sedimentation, organic matter, bulk density and particle density analysis. Due to the scale of this experiment and the homogeneity of the soil-vegetation components (Güntner and Bronstert, 2004) we divided the areas in two sets based on grain-size distribution, organic matter and bulk density. Gully 1 (G1) has specific features and comprises the first soil (S1), whereas gullies G2 and G3, close to each other, are represented by the second soil (S2). The soils are loamy, with clay content ranging from 6 % to 37 %. The particle density is  $2580 \text{ kg m}^{-3}$ . The soils are Luvisols and have typical profile, with the top layer relatively poor in clay when compared to the layers below and with the regular occurrence of gravel at the surface. Furthermore, Luvisols are rich in active clay, which makes them prone to form cracks and macropores when dry (dos Santos et al., 2016), a process also documented in soils with similar texture in a semiarid area in Spain (van Schaik et al., 2014). Rill erodibility values ( $K_r$ ) and critical shear stress ( $\tau_c$ ) for the soils were obtained using the Equations 1 and 2 (Alberts et al., 1995) and are also presented in Table 1.

$$K_r = 0.00197 + 0.00030\%VFS + 0.038633e^{(-1.84\%OM)} \quad (1)$$

$$\tau_c = 2.67 + 0.065\%C - 0.058\%VFS \quad (2)$$

where %VFS is the percentage of very fine sand, %C is the percentage of clay and %OM is the percentage of organic matter.

### 2.4 Rainfall data

Daily rainfall data for the location covering the entire period was provided by the Meteorological Service of Ceará (Funceme, 2018). We used of five rain-gauge stations in the region, covering the period from 1958 to 2015. The double mass method was employed to check data consistency (Supplementary material - Fig. S1). The gaps in the measurements (January 1958 and September 1960) were filled by the nearest gauging station. The annual rainfall in the area averages 613 mm (Supplementary material - Fig. S2) and its coefficient of variation is 43%, typical values for the Brazilian Semiarid Region (de Araújo and Piedra, 2009).

The modelling of the erosion processes is based on peak discharge, which demands sub-daily rainfall data, but only daily precipitation is available inside the study basin. To accomplish the modelling, correlation curves were used, from the Aiuaba Experimental Basin's (AEB) detailed hydrographs, which have been monitored since 2005 (Figueiredo et al., 2016). This

**Table 1.** Grain-size distribution, organic matter for both soils (S1 - for the gully 1 - and S2 - for the gullies 2 and 3) at three depths (10, 30 and 50 centimetres) and the respective texture classification (USDA); and the estimated (in italic) rill erodibility ( $K_r$ ) and critical shear stress ( $\tau_c$  of the site soils) obtained using Equations 1 and 2.

Soil and layer	Gravel > 2 mm	FCS <sup>a</sup> > 0.1 mm	VFS <sup>b</sup> > 0.05 mm	Silt > 0.002 mm	Clay < 0.002 mm	Organic Matter	Bulk density (kg m <sup>-3</sup> )	Soil Class	$K_r$ (s.m <sup>-1</sup> )	$\tau_c$ (Pa)
S1-10	13 %	45 %	21 %	11 %	10 %	3.1 %	1699	Sandy Loam	<i>0.015</i>	<i>2.102</i>
S1-30	6 %	46 %	16 %	14 %	18 %	3.3 %	1677	Sandy Loam	<i>0.016</i>	<i>2.912</i>
S1-50	4 %	63 %	20 %	7 %	6 %	2.2 %	1765	Loamy Sand	<i>0.020</i>	<i>1.900</i>
S2-10	17 %	33 %	22 %	11 %	17 %	4.9 %	1509	Sandy Loam	<i>0.012</i>	<i>2.499</i>
S2-30	8 %	29 %	6 %	20 %	37 %	5.7 %	1572	Clay Loam	<i>0.011</i>	<i>4.611</i>
S2-50	2 %	28 %	15 %	20 %	25 %	1.4 %	1643	Loam	<i>0.014</i>	<i>3.425</i>

<sup>a</sup> Fine to Coarse Sand; <sup>b</sup> Very Fine Sand.

experimental basin is located 190 km south of MRB, but both basins are climatically homogeneous (Mendes, 2010). Figure 4 shows the rainfall data for the MRB collected during the rainy season in 2019 (January to July). We can observe that the data has similar behaviour but constantly on the lower area of the plot. It is relevant to note that the year of 2019 in MRB was dry and such behaviour is expected. To obtain discharge values from intensity we used the SCS-CN method (Chow, 1959). For the modelling effort, the main variables are the event peak discharge and its respective duration. Because the gully catchment areas are very small, their respective concentration time is negligible compared with the intense-rainfall duration in the region (Figueiredo et al., 2016), yielding a uniform pattern of peak discharge. For each event, four intensities were assessed: average ( $I_{av}$ ), sixty-minute maximum ( $I_{60}$ ), thirty-minute maximum ( $I_{30}$ ) and fifteen-minute maximum ( $I_{15}$ ) intensities. Figure 4 also depicts the correlation curves between daily precipitation and event duration, as well as those between daily precipitation and rainfall intensity at the Aiuaba Experimental Basin.

## 2.5 Coupled Model (FL-SM)

The proposed model, hereafter addressed as FL-SM, was designed to model small permanent gullies based on the coupling of the models of Foster and Lane (1983) and Sidorchuk (1999) further described bellow. The model proposed uses the equations of Foster and Lane for calculating the cross-section area and geometry over many events. The eroded layers, obtained for each erosive event, are piled and summed. While the Foster and Lane Model was applicable for single events generating rectangular-shaped sections, this model adaptation allows us to calculate the section geometry for long term gullies. The model inserts a routine for wall erosion based on the equations proposed by Sidorchuk, which are implemented once the gully reaches a threshold. This threshold is related to the cross-section area and catchment geometry. Once this threshold is attained, the equations of Sidorchuk are used for estimating the channel cross-section growth based on wall erosion. A flow chart of the model can be found in the supplementary material (Fig. S3).



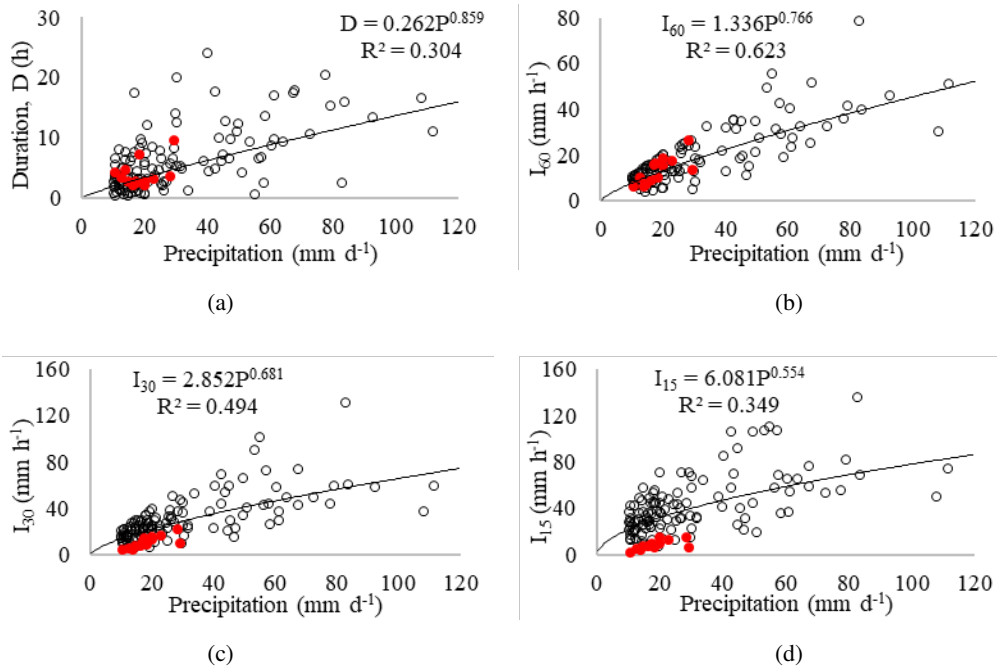


**Figure 4.** Correlation between daily precipitation and sub-daily variables at the Aiuaba Experimental Basin (Figueiredo et al., 2016). (a) daily precipitation versus event duration ( $D$ ); (b) daily precipitation versus 60-minute maximum intensity ( $I_{60}$ ); (c) daily precipitation versus 30-minute maximum intensity ( $I_{30}$ ); and (d) daily precipitation versus 15-minute maximum intensity ( $I_{15}$ ). The white circles indicate data obtained in Aiuaba from 2005 to 2014. The red dots indicate precipitations measured in the MRB from January to July 2019 (rainy season).

### 2.5.1 The Foster and Lane Model (FLM)

160 The Foster and Lane (1983) ephemeral-gully model aims at explaining “erosion by concentrated flow in farm fields” for single runoff intensive events. The gullies are considered ephemeral as productive farmlands usually provide periodic tillage to diminish or remove completely the gullies generated by previous events. The model is physically based, uses the Manning equation, mass balance, and shear stress mobilization; it assumes an equilibrium channel width and the gully evolution in two steps. The first step is the vertical incision, when the concentrated overflow starts digging the channel with a constant width.

165 The second step starts after the bottom of the channel reaches a non-erodible layer. Then, the section starts a sideward erosive process, widening until the end of the effective runoff, i.e., that with a shear stress below the critical stress. Detachment ratio ( $D_r$ ) and shear stress ( $\tau$ ) are given by the Equations (3) and (4).

$$D_r = K_r (\tau - \tau_c) \quad (3)$$

$$170 \quad \tau(X) = 1.35\gamma R_h S \left[ 1 - \left( 1 - 2 \frac{X}{WP} \right)^{2.9} \right] \quad (4)$$

In Equation 4,  $X$  is the position of a point on the channel bed, varying from zero to WP (wet perimeter).  $S$  is the longitudinal slope of the channel;  $R_h$  the hydraulic radius; and  $\gamma$  is the specific gravity of water (assumed  $9.81 \text{ kN m}^{-3}$ ).

In order to be able to model long-term gullies using Foster and Lane (1983) equations, the following assumptions were made: first, all mobilized sediment is carried away by the discharges, i.e., there is no sediment deposition on the channel bed.

175 This assumption was confirmed by field surveys in many sections, where very little loose sediment was identified. Secondly, in the long run, the effect of each intense runoff can be piled in a cumulative model of widths/depths layers. This implies that each erosive event does not suffer significant influence of the previous, and the total eroded soil is related only with the energy of each event. The piling process considered all events with runoff. Flow charts for the original Foster and Lane Model and how it allows to model multiple events by piling area available in the supplementary material (Fig. S4 and S5).

180 To estimate the effect of wall erosion at the studied site, we first proposed an empirical parameter ( $\lambda$  – Eq. 5) to correct the effect of lateral flow and wall erosion. This multiplicative parameter was calibrated and validated as function of the catchment shape, based on two coefficients: the Gravelius coefficient ( $K_G$  – Eq. 6) and the form coefficient ( $K_F$  – Eq. 7). Both coefficients describe the geometry of the catchment area and can be interpreted as how compact the area distribution is. Commonly linked to flood proneness, these parameters also relate to the transversal distance of the catchment area, which influences the amount

185 of lateral inflow into the mainstream. The diagrams of  $\lambda$  versus both parameters are presented in Figure 5. Two equations [ $\lambda(K_G)$  and  $\lambda(K_F)$ , see Figure 5] were calibrated using data from 14 randomly selected sections out of the 21 assessed by the DEM. The remaining data (from seven sections) were used to validate the equations.

$$\lambda = \frac{A_o}{A_m} \quad (5)$$

$$K_G = 0.28 \cdot \frac{C_P}{C_A} \quad (6)$$

190  $K_F = \frac{C_A}{C_L^2} \quad (7)$

In Equation 5 the terms  $A_o$  and  $A_m$  are the observed and measured cross-section area and in Equations 6 and 7,  $C_P$ ,  $C_A$  and  $C_L$  stand for the catchment perimeter, area and length, respectively.

$$\lambda = \max(5.859K_F^{0.707}; 1.0) \quad (8)$$

The coefficient ( $K_F$ ) yielded a positive Nash-Sutcliffe Efficiency value and smaller RMSE (0.17 and 0.67 respectively), which did not occur with the Gravelius coefficient (-2.43 and 0.84 respectively). In the revised model, hereafter addressed as FLM- $\lambda$ , the FLM area output is multiplied by the calibrated parameter  $\lambda$  (Equation 8), yielding the eroded area. Applying this factor caused a significant improvement in model efficiency, with NSE increasing from 0.557 to 0.757. The incremental area

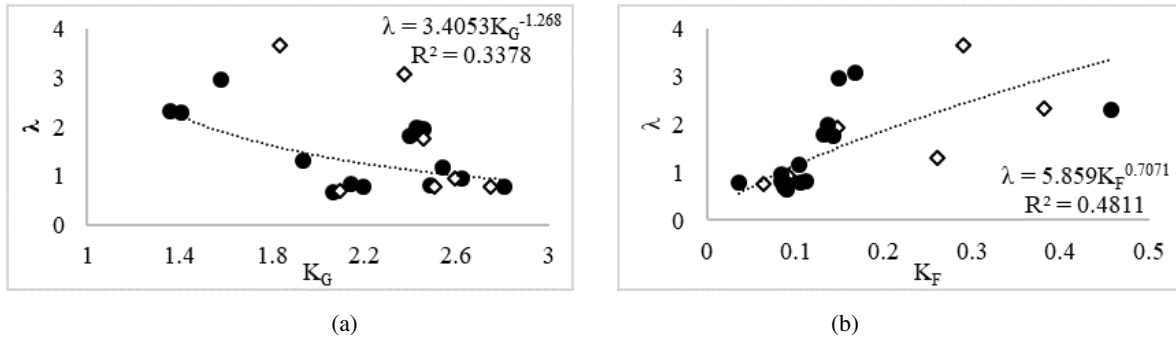


**Figure 5.** Correlations between the ratio ( $\lambda = A_o/A_m$ ) and (a) the Gravelius coefficient ( $K_G$ ) and (b) the form factor ( $K_F$ ) for 21 monitored cross-sections at MRB. Black dots refer to calibration cross-sections and white diamonds refer to validation cross-sections. The values of  $R^2$  indicated in the plots are for the calibration. The validation  $R^2$  were 0.10 for  $K_G$  and 0.54 for  $K_F$ .

produced by the multiplication of  $\lambda$  is assumed to increase the width of the upper half of the cross-section, keeping bottom width and the orthogonality of the walls unchanged.

## 200 2.5.2 The Sidorchuk Model (SM)

The Sidorchuk model (Sidorchuk, 1999) is physically and empirically based. It considers mass balance of sediment, shear stress (in terms of critical velocity), soil cohesion and the Manning equation to estimate the cross-section geometry and channel slope. It also uses empirical equations based on field measurement to estimate the flow depth and width. The model gives special attention to the processes involving gully wall transformation, as shown in Equations (9) and (10).

$$205 \quad D_{vcr} = \frac{2C_h}{g \rho_s} \cos(\varphi) \sin^{-2} \left[ \frac{1}{2} \left( \varphi + \frac{\pi}{2} \right) \right] \quad (9)$$

$$\frac{C_h}{g \rho_s D_v} = \frac{\rho_s - w\rho}{\rho} \tan \varphi \cos^2 \phi - \frac{\sin 2\phi}{2} \quad (10)$$

In Equations (9) and (10),  $C_h$  is soil cohesion (MPa);  $D_v$  the depth incision (m);  $D_{vcr}$  the critical value of depth for wall failure;  $w$  is the volumetric soil water content;  $\rho_s$  is the bulk density of the soil;  $\rho$  is the density of water;  $g$  is the gravity acceleration;  $\varphi$  is the soil internal friction angle; and  $\phi$  is the wall slope, in degrees.

## 210 2.5.3 Threshold definition

The FL-SM requires the determination of a threshold value for the implementation of the wall erosion equations. Such a threshold controls when the wall erosion becomes significant for the total amount of eroded soil. In the model, it represents the limit stage, above which Sidorchuk (1999) equations are used. It also represents the scale when solely the channel bed erosion,

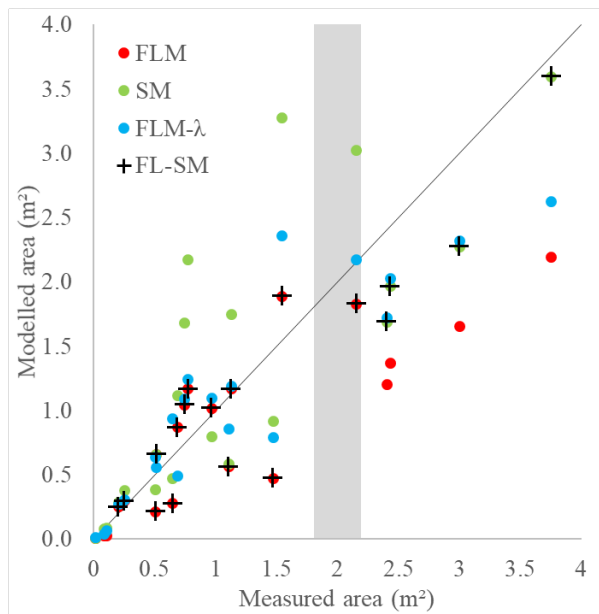


**Figure 6.** Performance of the coupled model (FL-SM), Foster and Lane Model (FLM and FLM- $\lambda$ ) and the Sidorchuk model (SM).

described by the Foster and Lane (1983) equations start to consistently underestimate the measured area. In this study we used the Foster and Lane model to identify this scale where the both processes (channel bed and wall erosion) switch relevance.

## 2.6 Model fitness evaluators

To assess the goodness-of-fit, the Nash and Sutcliffe (1970) efficiency coefficient (NSE); the root mean square error (RMSE); and the percent bias (PBIAS) were used (see Moriasi et al. (2007)). Besides, the methodology proposed by Ritter and Muñoz-Carpena (2013) asserts statistical significance to the evaluators. The proposed model is based on Monte Carlo sample techniques to reduce subjectivity when assessing the goodness-of-fit of models.

## 3 RESULTS

### 3.1 Coupled model (FL-SM)

The FL-SM presented a Nash-Sutcliffe Efficiency coefficient of 0.846 when using a threshold for the area of the cross-section of 2.2 m<sup>2</sup>. This value can be slightly improved if a parameter  $\lambda$  is calibrated for sections that are smaller than the threshold (FL-SM- $\lambda$ ), yielding a NSE of 0.853. fBy doing this, however, a calibrated parameter has to be reintroduced, which is not desired. Figure 6 presents the scatter of modelled and measured data for the models implemented. In Figure 7 some output examples for the sections above the threshold are presented.

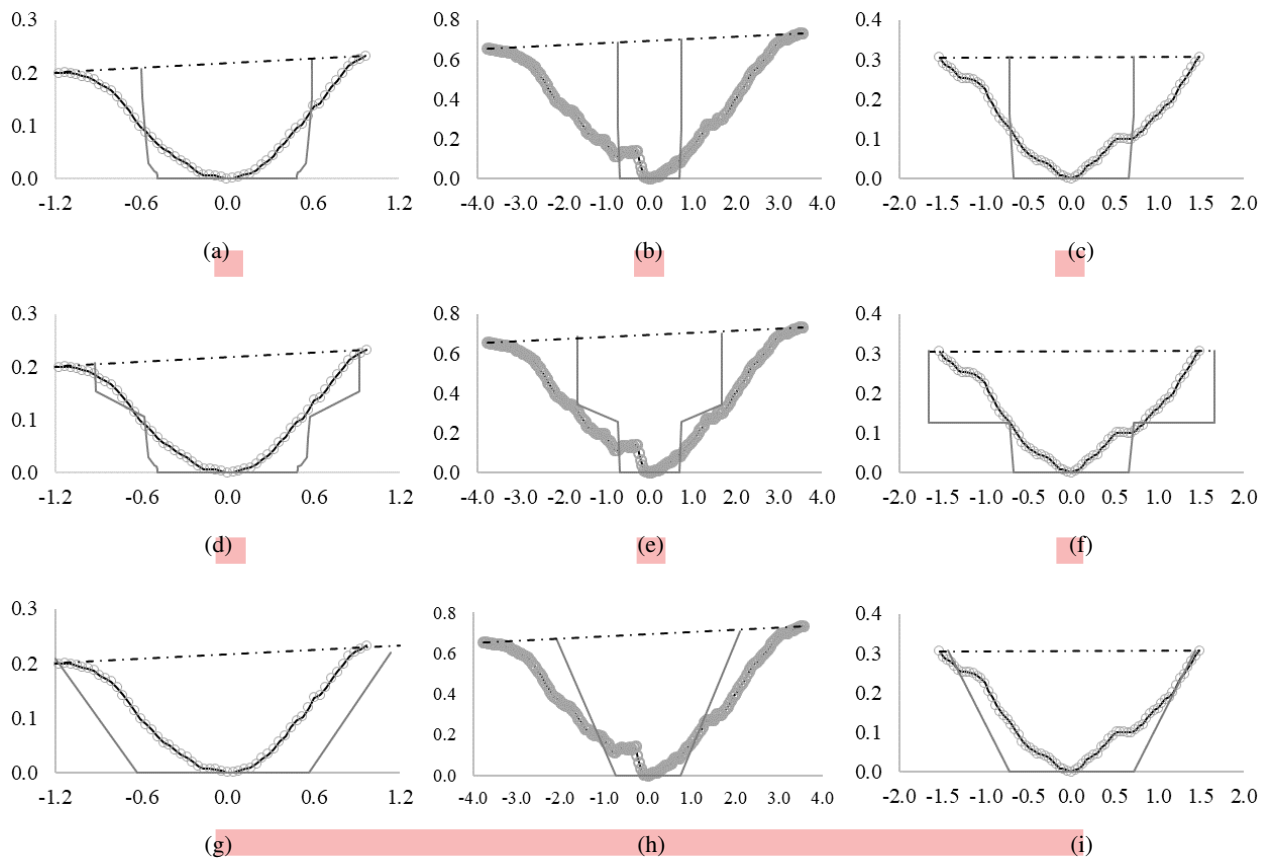


**Figure 7.** Some examples of gully cross-sections measured (black line with circles) and the modelled (dark grey line) geometry. figures (a), (b) and (c) show the output for the model of Foster and Lane; figures (d), (e) and (f) the output for the model of Foster and Lane adapted with the parameter  $\lambda$  and figures (g), (h) and (i) the result from the Sidorchuk Model (SM). Distances in metres. Section in (a, d and g) is a section obtained from gully 1, (b, e and h) from gully 2, and (c, f and i) from gully 3.

In terms of geometry, sections below the threshold have cross-sections similar to Figure 7 [(a), (b), (c)], with rectangular-like shape, unless the  $\lambda$  parameter is reintroduced, which leads to cross-sections like Figure 7 [(d), (e), (f)], with piled rectangles. When the area surpasses the threshold value, sections have mainly trapezoidal geometry, as illustrated in Figure 7 [(g), (h), (i)]. It is important to highlight that the model can produce triangular geometry, but none was obtained in this study.

### 3.1.1 Threshold analysis

The interpretation of the threshold for implementation of the wall erosion routine can be based on (a) the cross-section area or (b) the catchment geometry, as illustrated in Figure 8. The first approach considers a critical area that once reached marks when the wall erosion is really significant over the other processes. In this study the threshold identified was at an area of 2.2 m<sup>2</sup>. After that, the model calculates the effect of sidewall erosion and reaches the critical final area for the analysed section.

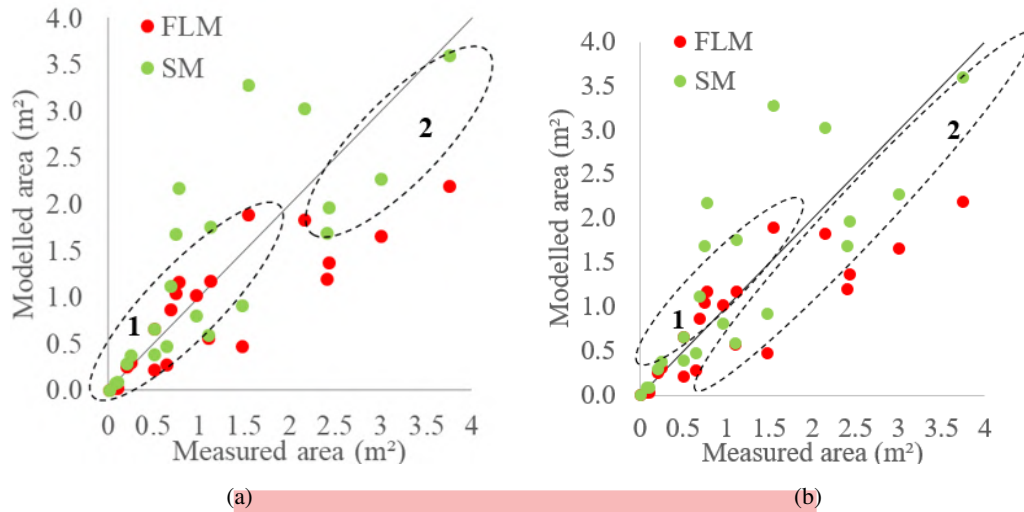


**Figure 8.** Thresholds for wall erosion: (a) based on the cross-section area; (b) based on the catchment geometry and  $K_F$ . In both plots the set 1 indicates the domain of bed erosion and Foster and Lane equations and set 2 the domain of wall erosion and Sidorchuk equations.

The presence of a threshold for applying the sidewall erosion routine indicates a change of relevance among processes on a given scale. Although the threshold is addressed as an area, this is only a consequence of more complex interactions among discharge, flow erosivity, cohesion and gravitational forces.

240 The second interpretation is related to the catchment geometry, as the approach given to the parameter  $\lambda$  also related to the  $K_F$ . From the distribution of the cross sections we can observe sections that are better modelled by SM even under the threshold. By analysing the values of form coefficient ( $K_F$ ) of each set (Figure 8b) we observed that set 1 has  $K_F$  of  $(0.08 \pm 0.02)$  and set 2 has  $0.22 (\pm 0.12)$ . Higher values of  $K_F$  indicate a more compact catchment, with more lateral flux into the channel, therefore producing more erosion in the soil. By sorting the model results of FLM and SM based in the form coefficient, using  
245 the threshold of  $K_F = 0.15$ , we obtained an NSE of 0.79.

### 3.1.2 Rainfall intensity

Of the three gullies, twenty-one cross sections with no interference of bushes or trees were selected from the Digital Elevation Model. The FLM was tested for the 60-minute, 30-minute, 15-minute and average intensities [ $FLM(I_{60})$ ,  $FLM(I_{30})$ ,  $FLM(I_{15})$ ,  $FLM(I_{av})$ ]. It showed the best response when using the thirty-minute intensity [ $FLM(I_{30})$ ; NSE = 0.557]. Figure 9 presents  
250 the plot of the model outputs for area and width compared with measured data. One can observe that no tested intensity gave a realistic approach to the observed values of width. Moreover, the model did not show good responses to the cross-section geometry, regardless of the intensity tested. This may indicate a flaw of the model concerning the sidewall erosive process. To enhance model performance, the focus was set on cross-section erosive processes. The FLM considers a rectangular shape for the sections, but the field survey showed that the sections are rather trapezoidal or triangularly shaped (Figure 10). Among the



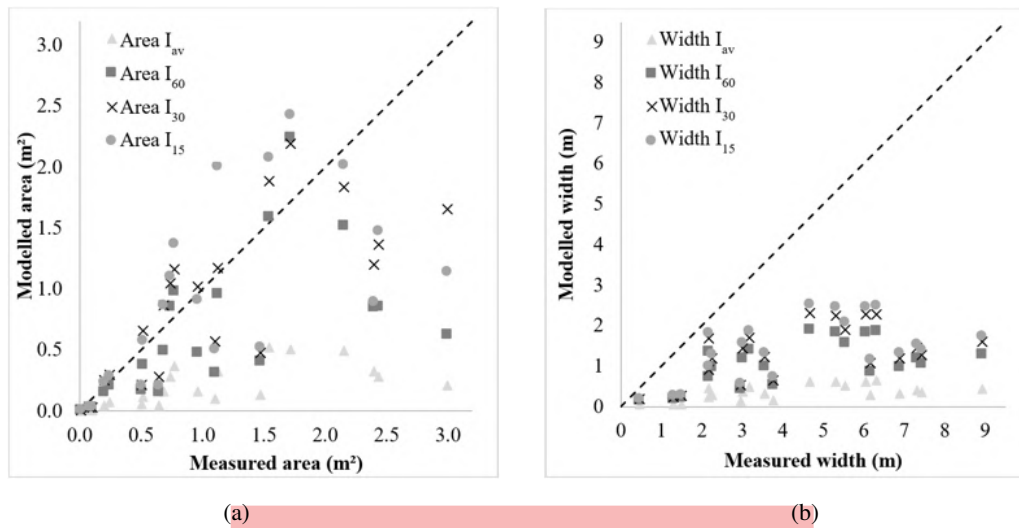


**Figure 9.** Results of the FLM for the different intensities ( $I_{av}$  – average;  $I_{60}$  – 60-min;  $I_{30}$  – 30-min; and  $I_{15}$  – 15-min) to generate the peak discharge. Scatter of points comparing measured and modelled values: (a) Area; (b) Top Width.

255 factors that can shape gully walls, there are seepage, slope material, and the slope angle itself (Bocco, 1991; Sidorchuk, 1999; Martínez-Casasnovas et al., 2004; Bingner et al., 2016). Besides, gully walls can be shaped by lateral discharge (Blong and Veness, 1982), which depends directly on the morphology of the cross-section catchment area. Figure 9 also shows a tendency of the model in underestimating the cross-section area, which implies that the model does not consider all the relevant erosive processes. The sidewall erosion has proven to be a relevant source material, often representing over 50 % of the eroded mass 260 (Crouch, 1987, 1990), whereas the FLM only assumes the vertical sidewall morphology. Hereafter the acronym FLM will refer solely to the model implemented with 30-minute intensity.

### 3.2 Model evaluators

The coupled model, FL-SM, presented the highest performance of goodness-of-fit evaluators (Figure 10a). The model yielded a PBIAS value below 10 %, which is very good. The coupled-model RMSE was also low (1.82), whereas the NSE reached a 265 value of 0.846, being classified as good (Ritter and Muñoz-Carpena, 2013) or very good (Moriassi et al., 2007).

Figure 10b shows the evolution of NSE values with more details so that conclusions can be drawn. The Foster and Lane model with  $\lambda$  parameter (FLM- $\lambda$ ) was calibrated with 14 cross-sections out of 21 and performed as well as the Sidorchuk model (SM), which considers the sidewall effect. For the coupled model, there is no efficiency gain when applying the calibrated parameter ( $\lambda$ ) to sections below threshold which indicates that the lateral inflow is only relevant for larger sections. 270 Another approach to estimate the goodness-of-fit of a model was proposed by Ritter and Muñoz-Carpena (2013). The routine (FITEVAL) consists of repeatedly resampling from the dataset and handles each resample as an actual sample of the population. This grants the generation of a confidence interval for statistical evaluators. The method classifies the model as acceptable to

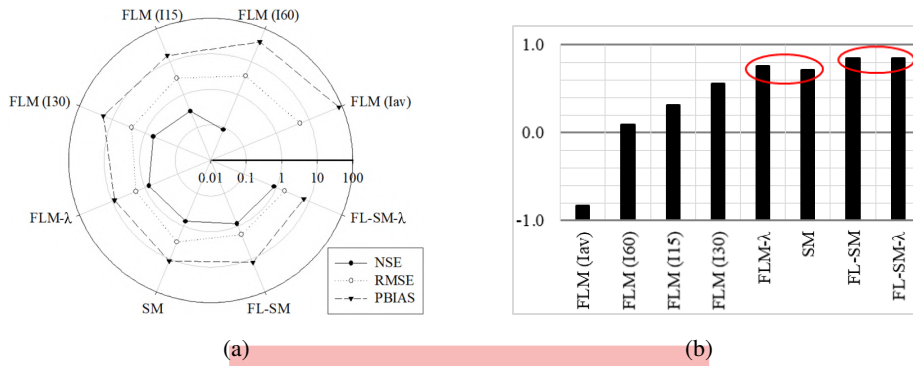


**Figure 10.** (a) Model evaluators NSE, RMSE and PBIAS. The web graphs shows the performance of all tested models – values of PBIAS in percentage. (b) Evolution of the NSE values for every model. The red balloons indicate models with similar efficiency. Values of PBIAS in percentage.

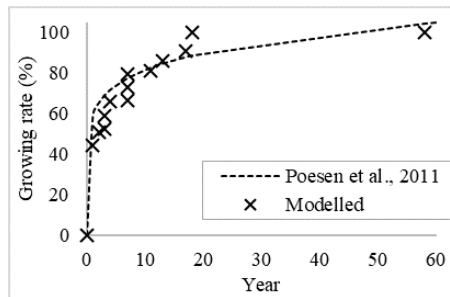


**Figure 11.** Behaviour of gully growing rate as proposed by literature (Poesen et al., 2011) and modelled (data from Gully 1).

very good –  $NSE \in [0.66;0.95]$  for a p-value of 0.05. A conservative interpretation of this result implies considering the lowest values as the minimum state of information, or as the one that contains (almost) no unproven hypothesis. As a consequence, and according to Ritter and Muñoz-Carpena (2013), the FL-SM can be classified as acceptable to very good. The detailed output of the FITEVAL analysis can be found in the supplementary material (Fig. S6).

### 3.3 Gully growing modelling

The model also mimics the growing dynamic of gullies and its latency periods between extreme events, as reported in literature (Vanwalleghe et al., 2005; Poesen et al., 2011; Poesen, 2018) and illustrated in Fig. 11. Gully growing is commonly described as being a fast process in the first years and then progressively slowing down its enlargement. In our model, the mechanism that produces this dynamic is event piling. It could be observed that after a particularly intense event, the channel is sufficiently wide, whereas less intense events produce only a shallow flow with low shear stress and, therefore, no erosion. Only when a more intense event than the last erosive one happens, there is erosion. A flow chart of the final model (Foster-Lane-Sidorchuk Model) is available in the supplementary material (Fig. S5).

### 285 3.4 Landscape development impacts on gully erosion

Gullies are scale-dependent phenomena and frequently related to thresholds due to their initiation, which is based on catchment area and slope (Poesen et al., 2003; Torri and Borselli, 2003; Torri and Poesen, 2014; Poesen, 2018). Both characteristics are directly linked to shear stress and stream power when using physical gully models. Montgomery and Dietrich (1992) argue that changes in landscape and the drainage system can lead to a larger occurrence of channelization and its impacts can be noticed  
290 faster. Torri and Poesen (2014) suggest a threshold for head development in gullies as conveyed in Equation 11.

$$S C_A^{0.38} > k \quad (11)$$

where  $S$  ( $\text{m m}^{-1}$ ) is the slope,  $C_A$  (ha) is the catchment area and  $k$  in a parameter for channel and gully initiation.

For croplands in tropical conditions, the proposed value of  $k$  is 0.042 (Torri and Poesen, 2014). For the gullies in the present study, however, a head development for values lower than half ( $k = 0.020$ ) and systematically lower than the field data of  
295 (Vandaele et al., 1996) could be observed. These findings suggest soil vulnerability of the gully erosion region. Considering that the three experimental sites were located next to a road, this disturbance triggered gully initiation and other actions may cause similar problems in the region, such as deforestation and forest fire. The road not only enlarged the total catchment area, it also increased its length. While relations between catchment length and area are well-established ( $L = b C_A^{0.49}$ ) with values of  $b$  varying from 1.78 to 2.02 (Montgomery and Dietrich, 1992; Sassolas-Serrayet et al., 2018), the present experiments found  
300  $b$  equalling 3.17. With a smoother surface and almost no meandering, road construction caused modifications that promoted more energetic flows on the gully head. Road construction has also been identified as potential factor for gully initiation in other areas of the Brazilian Semiarid Region, as in the Salitre Catchment, where large gullies started after construction of an unpaved rural road (Souza et al., 2016; da Silva and Rios, 2018).

## 4 DISCUSSION

### 305 4.1 Coupled model (FL-SM)

The FL-SM considers two sediment sources, channel bed and sidewall. Gullies are, however, complex systems with many sources and interactions. Headcut, sidewall erosion due to raindrops and piping were not considered in our modelling approach. Processes of infiltration, subsurface flow and transport capacity were also neglected and should be properly addressed in future works. Nevertheless, the FL-SM assumptions managed to mimic well the field measurements, which implies that, at least in this  
310 study, the neglected processes are of lower relevance or were considered indirectly. For instance, sidewall erosion by raindrops can be considered insignificant over the wall failure process considered by Sidorchuk (1999). In addition, it is important to notice that, by selecting the 30-minute intensity, a less intense interval might be overlooked that produces erosive discharge, too, and can, therefore, explain the remaining processes.

Despite the good results obtained from the modelling, the use of stochastic approaches (Knapen et al., 2007; Sidorchuk, 2005) should improve the performance of the model and introduction of other sources of sediment. This is also relevant for generalisation and modelling of classical gullies. In the same way, the introduction of processes as armouring and energy losses as proposed by Hairsine and Rose (1992) can be interpreted as probabilistic terms.

#### 4.1.1 Foster and Lane Model (FLM)

The first attempt for this study was to identify which was the best peak and duration of rainfall to be considered. Due to the timescale of this work, it was required to select a single parameter for all the events. Therefore, a relevant result from this work is the confirmation that the 30-minute intensity is the one that provides most information about gully erosion. Wischmeier and Smith (1978) proposed the product of total storm energy and the 30-minute intensity to “predict the long-time average soil loss in runoff”. The use of  $I_{30}$  for estimating event-related gully erosion was previously experimentally tested by Han et al. (2017). The authors had monitored a gully in the Loess Plateau in China for 12 years, registering 115 erosive rainfall events. They concluded that the product of 30-minute intensity and total precipitation ( $P I_{30}$ ) was the key parameter to estimate total soil loss. Our results corroborate with this.

Furthermore, by applying the  $I_{30}$  in this study in order to estimate peak discharge and duration, it is implied that all the energy necessary to initiate and develop a gully channel comes from the most intense 30 minutes. Due to the limited number of gullies, it is not straightforward that the  $I_{30}$  could be the most representative index for any situation. Peak discharge and critical rainfall duration are often central variables in gully models (Foster and Lane, 1983; Watson and Laflen, 1986; Hairsine and Rose, 1992; Sidorchuk, 1999; Gordon et al., 2007) and are related to erosion initiation parameters and thresholds, such as shear stress and stream power. This second factor has frequently been reported in literature as being more correlated with both laminar and linear erosion (Torri and Borselli, 2003; de Araújo, 2007; Nazari Samani et al., 2016; Bennett and Wells, 2019). Figure 9a shows the performance of the tested intensities. Although the model using the 15-minute intensity presented smaller PBIAS and RMSE, the results indicated a large scatter around average. The FLM was further improved by the addition of the calibrated parameter  $\lambda$  (FLM-  $\lambda$ ). This parameter is included to predict the effect of lateral discharges over wall erosion. Due to the significant improvement produced by its insertion, it could be understood that the original FLM fails to tackle this source of material (Blong and Veness, 1982; Crouch, 1987).

#### 4.1.2 Sidorchuk Model (SM)

The SM produced good results in this study, which were similar to those obtained by inserting a calibrated factor ( $\lambda$ ) in FLM. It is important to note that the original model used empirical correlations to determine width (Sidorchuk, 1999; Nachtergaele et al., 2002) and those were obtained for the Yamal basin. In the present study, we substituted this approximation for the width estimated by the FLM model, which permitted a more physical approach and increased the quality of the SM. The model was also capable to predict well the sidewall slope.

The model, however, showed a trend of overestimating smaller cross-sections (see Figure 6), mainly due to section geometry. When applied, the bottom width of the channel is considered to be the final width obtained by FLM. In larger sections, this

hypothesis holds, once the discharge is large enough to carry all soil produced by sidewall erosion. In smaller sections, part of the soil is deposited and produces a V or U shaped cross-section (Starkel, 2011).

## 4.2 Topographic data

350 In terms of accuracy and agility, a topographic survey with UAV exceeds the Digital Elevation Model and permits to measure sites within a few minutes. Conventional measurements, such as those with total station or profilometer, are more time consuming and do not grant better resolutions. The UAV accuracy, however, can be enhanced by performing flights in lower heights and more GCPs (Agüera-Vega et al., 2017; James et al., 2017), as well as by using high-end equipment, such as more robust UAVs and stabilizers. Total stations can also be used to improve the accuracy of ground control points (Mesas-Carrascosa et al., 2016). Given the scale of this study and the presented results of the models, the four-centimetre pixel represents a good resolution, since it combines good precision with affordable computational costs (Wang et al., 2016). The solution of UAV-based volume assessment is a good option for monitoring gully evolution (Marzolff and Poesen, 2009; Stöcker et al., 2015), allowing frequent surveys, e.g., after every intense rainfall event. Trees and bushes obscure topographic measurements if too close to the gully channel and/or too dense in the catchment. Thus, UAV monitoring is more reliable for gully sites in non-360 or meagre-vegetated areas and meadows, which combines with the conditions of this study, except for gully 3, where it was impossible to accurately measure the total erosion volume due to relatively dense vegetation. It was, however, possible to select a large enough number of sections (eight) at gully 3 to assess the total erosion volume. The topographic survey shows that the gully watersheds contain large parts in the road, indicating a modification of the drainage system and change of the catchment boundaries – both causes of gully initiation foreseen by Ireland et al. (1939) – due to road construction, which promoted intense runoff and triggered gullies. Impacts of road construction on gully formation were also observed in Ethiopia (Nyssen et al., 2002) and the USA (Katz et al., 2014). Considering such previous records in literature and the information collected with locals, the modelling considered 1958 as the start of gully erosion, coinciding with road construction.

## 4.3 Soil data

Though the three studied gullies are located in the same mesoscale basin, the Caatinga biome is known for its soil variability 370 (Güntner and Bronstert, 2004) and soil properties do differ among the gullies. However, only small changes of texture were observed in different depths, allowing an analysis based on average properties. Nevertheless, for deeper and/or more variable soils, the discretization of soil properties, and therefore parameters such as rill erodibility ( $K_r$ ) and critical shear stress ( $\tau_c$ ) can easily be taken into account. The good performance of the final model (FL-SM) also indicates that the WEPP equations for critical shear stress and rill erodibility (Eq. 1 and 2) can be used for the soils of the region. These equations were obtained 375 via regression curves from data collected on 34 plot areas in the USA with a wide range of textures, slopes, land use and land cover. The areas from the WEPP model possess different geological and climatological conditions from the soils in the Brazilian Semiarid Region; this is why local studies should be carried out, since empirical equations frequently have strong local character (Ghorbani-Dashtaki et al., 2016; Dionizio and Costa, 2019).

#### 4.4 Rainfall data

380 This study shows that sub daily information of rainfall is of crucial importance for gully modelling. In this study, we used correlation curves based on long-term time series of a similar catchment in the region. However, such analysis might introduce an averaged and monotonic behaviour for the intensities, as illustrated in Figure 4, and is, therefore, unrealistic. Stochastic models should be tested to estimate sub daily information from daily rainfall. The estimation of discharge from rainfall can also be improved by considering water content in the soil and modelling its evolution over the studied period using water  
385 balance models.

#### 5 Conclusions

In this study, efforts were concentrated on understanding how the cross-section of small permanent gullies (with no groundwater contributions) evolve. It was possible to identify two main mechanisms: the first is bed erosion, governed by shear stress at the bottom of the channel. The second is the sidewall erosion due to gravitational processes and lateral flow. To successfully model  
390 both components, two models were coupled – those by Foster and Lane (1983) and Sidorchuk (1999). The two mechanisms, however, do not happen simultaneously in all sections, they depend on the process scale and are ruled by a threshold of eroded cross-section area. To model the gullies in a region without local data of sub-daily rainfall, correlation curves were used to estimate rain intensity from total daily precipitation. For the purpose of modelling peak discharges, the intensity that showed the best results was the 30-minute one ( $I_{30}$ ).

395 Gully is an erosion related to many processes and it is scale dependent. The attempt of proposing a generalist model for gullies should also consider these different scales and mechanisms involved in different stages of the gully development. Catchment shape and lateral flow have a central role on gully erosion and their influence should be further investigated. Infrastructure constructions, as roads, change conditions for gully initiation and was the trigger for the studied gullies.

The proposed final model (FL-SM; standing for Foster & Lane and Sidorchuk Model) presented a performance that varied  
400 from acceptable to very good, depending on the criteria. This model managed to estimate total erosion in a small permanent gully for a total period of six decades. Despite the good results of FL-SM, more efforts should be undertaken to tackle other sources of gully sediments, such as headcut and piping.

*Code and data availability.* Code and data available in the link: <https://github.com/PedroAlencarTUB/GullyModel-FLSM>

*Author contributions.* Alencar worked on fieldwork, programming, laboratory analysis. Teixeira carried image acquisition and processing.  
405 de Araújo acted as supervisor of the work and in its conceptualization. Alencar prepared the text with contributions of all authors.



*Competing interests.* The authors declare that they have no conflict of interest.

This work is part of the PhD work of **Pedro Alencar** and will be used in his dissertation.

*Disclaimer.*

*Acknowledgements.* This study was partly financed by the *Coordenação de Aperfeiçoamento de Pessoal de Nível Superior - Brasil (CAPES)* 410 - Finance Code 001 and by the *Edital Universal CNPq* - number 407999/2016-7. Pedro Alencar is funded by the DAAD. Many thanks to Prof. Eva Paton for the support and advising at the Technische Universität Berlin.

## References

- Agüera-Vega, F., Carvajal-Ramírez, F., and Martínez-Carricondo, P.: Assessment of photogrammetric mapping accuracy based on variation ground control points number using unmanned aerial vehicle, *Measurement*, 98, 221–227, 2017.
- 415 Albers, E. E., Nearing, M. A., Weltz, M. A., Risse, L. M., Pierson, F. B., Zhang, X. C., Lafren, J. M., and Simanton, J. R.: Soil Component, Tech. Rep. July, USDA, 1995.
- Alonso, C. V., Bennett, S. J., and Stein, O. R.: Predicting head cut erosion and migration in concentrated flows typical of upland areas, *Water Resources Research*, 38, 39–1–39–15, <https://doi.org/10.1029/2001wr001173>, 2002.
- Arabameri, A., Rezaei, K., Pourghasemi, H. R., Lee, S., and Yamani, M.: GIS-based gully erosion susceptibility mapping: a comparison among three data-driven models and AHP knowledge-based technique, *Environmental Earth Sciences*, <https://doi.org/10.1007/s12665-018-7808-5>, 2018.
- 420 Arabameri, A., Cerda, A., and Tiefenbacher, J. P.: Spatial Pattern Analysis and Prediction of Gully Erosion Using Novel Hybrid Model of Entropy-Weight of Evidence, *Water*, 11, 1129, 2019.
- Ascough, J. C., Baffaut, C., Nearing, M. A., and Liu, B. Y.: The WEPP watershed model .1. Hydrology and erosion, *Transactions of the Asae*, 40, 921–933, 1997.
- 425 Azareh, A., Rahmati, O., Rafiei-Sardooi, E., Sankey, J. B., Lee, S., Shahabi, H., and Ahmad, B. B.: Modelling gully-erosion susceptibility in a semi-arid region, Iran: Investigation of applicability of certainty factor and maximum entropy models, *Science of the Total Environment*, <https://doi.org/10.1016/j.scitotenv.2018.11.235>, 2019.
- Bennett, S. J. and Wells, R. R.: Gully erosion processes, disciplinary fragmentation, and technological innovation, *Earth Surface Processes and Landforms*, 44, 46–53, <https://doi.org/10.1002/esp.4522>, 2019.
- 430 Bernard, J., Lemunyon, J., Merkel, B., Theurer, F., Widman, N., Bingner, R., Dabney, S., Langendoen, E., Wells, R., and Wilson, G.: Ephemeral Gully Erosion — A National Resource Concern., U.S. Department of Agriculture. NSL Technical Research Report No. 69, p. 67 pp, 2010.
- Bingner, R. L., Wells, R. R., Momm, H. G., Rigby, J. R., and Theurer, F. D.: Ephemeral gully channel width and erosion simulation technology, *Natural Hazards*, 80, 1949–1966, <https://doi.org/10.1007/s11069-015-2053-7>, 2016.
- 435 Blong, R. J. and Veness, J. A.: The Role of Sidewall Processes in Gully Development, *Earth Surface Processes and Landforms*, 7, 381–385, 1982.
- Bocco, G.: Gully erosion: Processes and models, *Progress in Physical Geography*, 15, 392–406, 1991.
- Borrelli, P., Robinson, D. A., Fleischer, L. R., Lugato, E., Ballabio, C., Alewell, C., Meusburger, K., Modugno, S., Schütt, B., Ferro, V., Bagarello, V., Oost, K. V., Montanarella, L., and Panagos, P.: An assessment of the global impact of 21st century land use change on soil erosion, *Nature Communications*, 8, <https://doi.org/10.1038/s41467-017-02142-7>, 2017.
- 440 Castillo, C. and Gómez, J. A.: A century of gully erosion research: Urgency, complexity and study approaches, *Earth-Science Reviews*, 160, 300–319, <https://doi.org/10.1016/j.earscirev.2016.07.009>, 2016.
- Castillo, C., James, M. R., Redel-Macías, M. D., Pérez, R., and Gómez, J. A.: SF3M software: 3-D photo-reconstruction for non-expert users and its application to a gully network, *Soil*, 1, 583–594, <https://doi.org/10.5194/soil-1-583-2015>, 2015.
- 445 Chow, V. T.: *Open-channel hydraulics*, in: *Open-channel hydraulics*, McGraw-Hill, 1959.
- Coelho, C., Heim, B., Foerster, S., Brosinsky, A., and de Araújo, J. C.: In situ and satellite observation of CDOM and chlorophyll-a dynamics in small water surface reservoirs in the brazilian semiarid region, *Water (Switzerland)*, 9, <https://doi.org/10.3390/w9120913>, 2017.

- Crouch, R. J.: The relationship of gully sidewall shape to sediment production, *Australian Journal of Soil Research*, 25, 531–539, 1987.
- 450 Crouch, R. J.: Erosion processes and rates for gullies in granitic soils bathurst, new south wales, australia, *Earth Surface Processes and Landforms*, 15, 169–173, <https://doi.org/10.1002/esp.3290150207>, 1990.
- da Silva, A. J. P. and Rios, M. L.: *Alerta de desertificação no médio curso do Rio Salitre, afluente do Rio São Francisco*, Tech. rep., IFBA, Senhor do Bonfim, Bahia, 2018.
- Dabney, S. M., Vieira, D. A. N., Yoder, D. C., Langendoen, E. J., Wells, R. R., and Ursic, M. E.: Spatially Distributed Sheet, Rill, and  
455 Ephemeral Gully Erosion, *Journal of Hydrologic Engineering*, 20, C4014 009, 2015.
- de Araújo, J. C.: Entropy-based equation to assess hillslope sediment production, *Earth Surface Processes and Landforms*, 32, 2005–2018, <https://doi.org/10.1002/esp.1502>, 2007.
- de Araújo, J. C. and Piedra, J. I. G.: Comparative hydrology: analysis of a semiarid and a humid tropical watershed, *Hydrological Process*, 23, 1169–1178, <https://doi.org/10.1002/hyp>, 2009.
- 460 de Araújo, J. C., Güntner, A., and Bronstert, A.: Loss of reservoir volume by sediment deposition and its impact on water availability in semiarid Brazil / Perte de volume de stockage en réservoirs par sédimentation et impact sur la disponibilité en eau au Brésil semi-aride  
Loss of reservoir volume by se, *Hydrological Sciences Journal*, 51, 157–170, <https://doi.org/10.1623/hysj.51.1.157>, 2006.
- De Vente, J., Poesen, J., Verstraeten, G., Govers, G., Vanmaercke, M., Van Rompaey, A., Arabkhedri, M., Boix-fayos, C., Vente, J. D., Poesen, J., Verstraeten, G., Govers, G., Vanmaercke, M., Rompaey, A. V., Arabkhedri, M., and Boix-fayos, C.: Predicting soil erosion and sediment  
465 yield at regional scales: Where do we stand?, *Earth-Science Reviews*, 127, 16–29, <https://doi.org/10.1016/j.earscirev.2013.08.014>, 2013.
- Dionizio, E. A. and Costa, M. H.: Influence of Land Use and Land Cover on Hydraulic and Physical Soil Properties at the Cerrado Agricultural Frontier, *Agriculture*, 9, 14, <https://doi.org/10.3390/agriculture9010024>, 2019.
- dos Santos, J. C. N., de Andrade, E. M., Guerreiro, M. J. S., Medeiros, P. H. A., de Queiroz Palácio, H. A., and de Araújo Neto, J. R.: Effect of dry spells and soil cracking on runoff generation in a semiarid micro watershed under land use change, *Journal of Hydrology*, 541,  
470 1–10, <https://doi.org/10.1016/j.jhydrol.2016.08.016>, 2016.
- Figueiredo, J. V., Araújo, J. C., Medeiros, P. H. A., and Costa, A. C.: Runoff initiation in a preserved semiarid Caatinga small watershed, Northeastern Brazil, *Hydrological Processes*, 30, 2390–2400, <https://doi.org/10.1002/hyp.10801>, 2016.
- Foster, G. R. and Lane, L. J.: Erosion by concentrated flow in farm fields, in: D.B. Simons Symposium on Erosion and Sedimentation, p. 21, 1983.
- 475 Gaiser, T., Krol, M., Frischkom, H., and de Araujo, J. C., eds.: *Global Change and Regional Impacts*, Springer-Verlag, Berlin, [https://doi.org/10.1007/978-3-642-55659-3\\_9](https://doi.org/10.1007/978-3-642-55659-3_9), 2003.
- Ghorbani-Dashtaki, S., Homae, M., and Loiskandl, W.: Towards using pedotransfer functions for estimating infiltration parameters, *Hydrological Sciences Journal*, 61, 1477–1488, <https://doi.org/10.1080/02626667.2015.1031763>, 2016.
- Gordon, L. M., Bennett, S. J., Bingner, R. L., Theurer, F. D., and Alonso, C. V.: Simulating Ephemeral Gully Erosion in AnnAGNPS, Transactions of the ASAE, 50, 857–866, 2007.
- 480 Gudino-Elizondo, N., Biggs, T. W., Castillo, C., Bingner, R. L., Langendoen, E. J., Taniguchi, K. T., Kretschmar, T., Yuan, Y., and Liden, D.: Measuring ephemeral gully erosion rates and topographical thresholds in an urban watershed using unmanned aerial systems and structure from motion photogrammetric techniques, *Land Degradation and Development*, <https://doi.org/10.1002/ldr.2976>, 2018.
- Güntner, A. and Bronstert, A.: Representation of landscape variability and lateral redistribution processes for large-scale hydrological modelling in semi-arid areas, *Journal of Hydrology*, 297, 136–161, <https://doi.org/10.1016/j.jhydrol.2004.04.008>, 2004.
- 485

- Hairsine, P. B. and Rose, C. W.: Modeling water erosion due to overland flow using physical principles: 2. Rill flow, *Water Resources Research*, 28, 245–250, <https://doi.org/10.1029/91WR02381>, 1992.
- Han, Y., li Zheng, F., and meng Xu, X.: Effects of rainfall regime and its character indices on soil loss at loessial hillslope with ephemeral gully, *Journal of Mountain Science*, 14, 527–538, <https://doi.org/10.1007/s11629-016-3934-2>, 2017.
- 490 Hunke, P., Mueller, E. N., Schröder, B., and Zeilhofer, P.: The Brazilian Cerrado: Assessment of water and soil degradation in catchments under intensive agricultural use, *Ecohydrology*, 8, 1154–1180, <https://doi.org/10.1002/eco.1573>, 2015.
- Ireland, H., Sharpe, C. F. S., and Eargle, D. H.: *Principles of Gully Erosion in the Piedmont of South Carolina*, Tech. rep., USDA, Washington, 1939.
- James, M. R., Robson, S., Oleire-Oltmanns, S., and Niethammer, U.: Geomorphology Optimising UAV topographic surveys processed with  
495 structure-from-motion : Ground control quality , quantity and bundle adjustment, *Geomorphology*, 280, 51–66, 2017.
- Katz, H. A., Daniels, J. M., and Ryan, S.: Slope-area thresholds of road-induced gully erosion and consequent hillslope-channel interactions, *Earth Surface Processes and Landforms*, 39, 285–295, <https://doi.org/10.1002/esp.3443>, 2014.
- Knapen, A., Poesen, J., Govers, G., Gyssels, G., and Nachtergaele, J.: Resistance of soils to concentrated flow erosion: A review, *Earth-Science Reviews*, 80, 75–109, 2007.
- 500 Li, Q., Liu, G. B., Zhang, Z., Tuo, D. F., ru Bai, R., and fang Qiao, F.: Relative contribution of root physical enlacing and biochemical exudates to soil erosion resistance in the Loess soil, *Catena*, 153, 61–65, <https://doi.org/10.1016/j.catena.2017.01.037>, 2017.
- Liu, J., Nakatani, K., and Mizuyama, T.: Hazard mitigation planning for debris flow based on numerical simulation using Kanako simulator, *Journal of Mountain Science*, 9, 529–537, <https://doi.org/10.1007/s11629-012-2225-9>, 2012.
- Liu, X. L., Tang, C., Ni, H. Y., and Zhao, Y.: Geomorphologic analysis and a physico-dynamic characteristics of Zhatai-Gully debris flows  
505 in SW China, *Journal of Mountain Science*, 13, 137–145, 2016.
- Maetens, W., Vanmaercke, M., Poesen, J., Jankauskas, B., Jankauskiene, G., and Ionita, I.: Effects of land use on annual runoff and soil loss in Europe and the Mediterranean: A meta-analysis of plot data, *Progress in Physical Geography*, 36, 599–653, <https://doi.org/10.1177/0309133312451303>, 2012.
- Martínez-Casasnovas, J. A., Ramos, M. C., and Poesen, J.: Assessment of sidewall erosion in large gullies using multi-temporal DEMs and  
510 logistic regression analysis, *Geomorphology*, 58, 305–321, <https://doi.org/10.1016/j.geomorph.2003.08.005>, 2004.
- Marzolff, I. and Poesen, J.: Geomorphology The potential of 3D gully monitoring with GIS using high-resolution aerial photography and a digital photogrammetry system, *Geomorphology*, 111, 48–60, <https://doi.org/10.1016/j.geomorph.2008.05.047>, 2009.
- Mendes, F. J.: *Uma Proposta de Reclassificação das Regiões Pluviometricamente Homogêneas do Estado do Ceará*, Dissertação, Universidade Estadual do Ceará, 2010.
- 515 Mesas-Carrascosa, F. J., García, M. D. N., De Larriva, J. E. M., and García-Ferrer, A.: An analysis of the influence of flight parameters in the generation of unmanned aerial vehicle (UAV) orthomosaicks to survey archaeological areas, *Sensors (Switzerland)*, 16, 2016.
- Molina, A., Govers, G., Van Den Putte, A., Poesen, J., and Vanacker, V.: Assessing the reduction of the hydrological connectivity of gully systems through vegetation restoration: Field experiments and numerical modelling, *Hydrology and Earth System Sciences*, 13, 1823–1836, <https://doi.org/10.5194/hess-13-1823-2009>, 2009.
- 520 Montenegro, S. and Ragab, R.: Impact of possible climate and land use changes in the semi arid regions: A case study from North Eastern Brazil, *Journal of Hydrology*, 434–435, 55–68, <https://doi.org/10.1016/j.jhydrol.2012.02.036>, 2012.
- Montgomery, D. and Dietrich, W.: *Channel Initiation and Problem of Landscape Scale*, *Science*, 255, 826–830, 1992.
- Montgomery, D. R.: *Dirt: The Erosion of Civilizations*, universit y of california press, Berkeley, 2007.

- Moriasi, D. N., Arnold, J. G., Van Liew, M. W., Bingner, R. L., Harmel, R. D., and Veith, T. L.: Model Evaluation Guidelines for Systematic Quantification of Accuracy in Watershed Simulations, *Transactions of the ASABE*, 50, 885–900, 2007.
- 525 Nachtergaele, J., Poesen, J., Steegen, A., Takken, I., Beuselinck, L., Vandekerckhove, L., and Govers, G.: The value of a physically based model versus an empirical approach in the prediction of ephemeral gully erosion for loess-derived soils, *Geomorphology*, 2001.
- Nachtergaele, J., Poesen, J., Sidorchuk, A., and Torri, D.: Prediction of concentrated flow width in ephemeral gully channels, *Hydrological Processes*, 16, 1935–1953, <https://doi.org/10.1002/hyp.392>, 2002.
- 530 Nash, E. and Sutcliffe, V.: River flow forecasting through conceptual models Part I – A discussion of principles, *Journal of Hydrology*, 10, 282–290, 1970.
- Nazari Samani, A., Chen, Q., Khalighi, S., James Wasson, R., and Rahdari, M. R.: Assessment of land use impact on hydraulic threshold conditions for gully head cut initiation, *Hydrology and Earth System Sciences*, 20, 3005–3012, <https://doi.org/10.5194/hess-20-3005-2016>, 2016.
- 535 Nearing, M., Pruski, F., and O’neal, M.: Expected climate change impacts on soil erosion rates: a review, *Journal of soil and water conservation*, 59, 43–50, 2004.
- Nkonya, E., Anderson, W., Kato, E., Koo, J., Mirzabaev, A., von Braun, J., and Meyer, S.: Global Cost of Land Degradation, in: *Economics of Land Degradation and Improvement - A Global Assessment for Sustainable Development*, edited by Nkonya, E., Mirzabaev, A., and von Braun, J., chap. 6, pp. 117–165, Springer Open, Cham, <https://doi.org/10.1007/978-3-319-19168-3>, 2016.
- 540 Nyssen, J., Poesen, J., Moeyersons, J., Luyten, E., Veyret-Picot, M., Deckers, J., Haile, M., and Govers, G.: Impact of Road Building on Gully Erosion Risk: a Case of Study from the Northern Ethiopian Highlands, *Earth Surface Processes and Landforms*, 27, 1267–1283, 2002.
- Panagos, P., Ballabio, C., Meusburger, K., Spinoni, J., Alewell, C., and Borrelli, P.: Towards estimates of future rainfall erosivity in Europe based on REDES and WorldClim datasets, *Journal of Hydrology*, 548, 251–262, <https://doi.org/10.1016/j.jhydrol.2017.03.006>, 2017.
- 545 Paton, E. N., Smetanová, A., Krueger, T., and Parsons, A.: Perspectives and ambitions of interdisciplinary connectivity researchers, *Hydrology and Earth System Sciences*, 23, 537–548, <https://doi.org/10.5194/hess-23-537-2019>, 2019.
- Pimentel, D., Harvey, C., Resosudarmo, P., Sinclair, K., Kurz, D., McNair, M., Crist, S., Shpritz, L., Fitton, L., Saffouri, R., et al.: Environmental and economic costs of soil erosion and conservation benefits, *Science*, 267, 1117–1123, 1995.
- Pineux, N., Lisein, J., Swerts, G., Biielders, C., Lejeune, P., Colinet, G., and Degré, A.: Can DEM time series produced by UAV be used to quantify diffuse erosion in an agricultural watershed?, *Geomorphology*, 280, 122–136, 2017.
- 550 Pinheiro, E. A. R., Costa, C. A. G., and Araújo, J. C. D.: Effective root depth of the Caatinga biome, *Arid Environments*, 89, 4, 2013.
- Pinheiro, E. A. R., Metselaar, K., de Jong van Lier, Q., and de Araújo, J. C.: Importance of soil-water to the Caatinga biome, Brazil, *Ecohydrology*, 9, 1313–1327, <https://doi.org/10.1002/eco.1728>, 2016.
- Poesen, J.: Soil erosion in the Anthropocene: Research needs, *Earth Surface Processes and Landforms*, 43, 64–84, <https://doi.org/10.1002/esp.4250>, 2018.
- 555 Poesen, J., Vandekerckhove, L., Nachtergaele, J., Oostwoud Wijdenes, D., Verstraeten, G., and Van Wesemael, B.: Gully Erosion in Dryland Environments, in: *Dryland Rivers : Hydrology and Geomorphology of Semi-Arid*, January, chap. 8, pp. 229–248, John Wiley & Sons, Ltd, 2002.
- Poesen, J., Nachtergaele, J., Verstraeten, G., and Valentin, C.: Gully Erosion and Environmental Change: Importance and Research Needs, *Catena*, 50, 91–133, [https://doi.org/10.1016/S0341-8162\(02\)00143-1](https://doi.org/10.1016/S0341-8162(02)00143-1), 2003.
- 560

- Poesen, J. W., Torri, D. B., and Van Walleghem, T.: Gully Erosion: Procedures to Adopt When Modelling Soil Erosion in Landscapes Affected by Gullyng, *Handbook of Erosion Modelling*, pp. 360–386, <https://doi.org/10.1002/9781444328455.ch19>, 2011.
- Ritter, A. and Muñoz-Carpena, R.: Performance evaluation of hydrological models : Statistical significance for reducing subjectivity in goodness-of-fit assessments, *Journal of Hydrology*, 480, 33–45, <https://doi.org/10.1016/j.jhydrol.2012.12.004>, 2013.
- 565 Ruljigaljig, T., Tsai, C.-j., Peng, W.-f., and Yu, T.-t.: Evaluating the influence of gully erosion on landslide hazard analysis triggered by heavy rainfall, in: *EGU 2017*, vol. 19, p. 1, 2017.
- Sander, G. C., Zheng, T., and Rose, C. W.: Update to "Modeling water erosion due to overland flow using physical principles: 1. Sheet flow", *Water Resources Research*, 43, 2–5, 2007.
- Sartori, M., Philippidis, G., Ferrari, E., Borrelli, P., Lugato, E., Montanarella, L., and Panagos, P.: A linkage between the biophysical and the economic: Assessing the global market impacts of soil erosion, *Land Use Policy*, 86, 299–312, 2019.
- 570 Sassolas-Serrayet, T., Cattin, R., and Ferry, M.: The shape of watersheds, *Nature Communications*, 9, 1–8, 2018.
- Sena, A., Barcellos, C., Freitas, C., and Corvalan, C.: Managing the health impacts of drought in Brazil, *International Journal of Environmental Research and Public Health*, 11, 10737–10751, <https://doi.org/10.3390/ijerph111010737>, 2014.
- Sidorchuk, A.: Dynamic and static models of gully erosion, *Catena*, 37, 401–414, [https://doi.org/10.1016/S0341-8162\(99\)00029-6](https://doi.org/10.1016/S0341-8162(99)00029-6), 1999.
- 575 Sidorchuk, A.: Stochastic components in the gully erosion modelling, *Catena*, 63, 299–317, 2005.
- Silva, E., Gorayeb, A., and de Araújo, J.: *Atlas socioambiental do Assentamento 25 de Maio-Madalena-Ceará*, Fortaleza: Ed. Expressão Gráfica, 2015.
- Souza, J. O., Correa, A. C., and Brierley, G. J.: An approach to assess the impact of landscape connectivity and effective catchment area upon bedload sediment flux in Saco Creek Watershed, Semiarid Brazil, *Catena*, 138, 13–29, 2016.
- 580 Starkel, L.: Paradoxes in the development of gullies, *Landform Analysis*, 17, 11–13, 2011.
- Stöcker, C., Eltner, A., and Karrasch, P.: Measuring gullies by synergetic application of UAV and close range photogrammetry - A case study from Andalusia, Spain, *Catena*, 132, 1–11, <https://doi.org/10.1016/j.catena.2015.04.004>, 2015.
- Storm, D. E., Barfield, B. J., and Ormsbee, L. E.: *Hydrology And Sedimentology Of Dynamic Rill Networks - Volume I - Erosion Model For Dynamic Rill Networks*, Tech. rep., University of Kentucky, Lexington, 1990.
- 585 Thompson, J. R.: Quantitative Effect of Watershed Variables on Rate of Gully-Head Advancement, *Transactions of the ASAE*, 7, 0054–0055, 1964.
- Torri, D. and Borselli, L.: Equation for high-rate gully erosion, *Catena*, 50, 449–467, [https://doi.org/10.1016/S0341-8162\(02\)00126-1](https://doi.org/10.1016/S0341-8162(02)00126-1), 2003.
- Torri, D. and Poesen, J.: A review of topographic threshold conditions for gully head development in different environments, *Earth Science Reviews*, 130, 73–85, <https://doi.org/10.1016/j.earscirev.2013.12.006>, 2014.
- 590 Valentin, C., Poesen, J., and Li, Y.: Gully erosion: Impacts, factors and control, *Catena*, 63, 132–153, 2005.
- van Schaik, N. L., Bronstert, A., de Jong, S. M., Jetten, V. G., van Dam, J. C., Ritsema, C. J., and Schnabel, S.: Process-based modelling of a headwater catchment in a semi-arid area: The influence of macropore flow, *Hydrological Processes*, 28, 5805–5816, 2014.
- Vandaele, K., Poesen, J. A. W., Govers, G., and van Wesemael, B.: Geomorphic threshold conditions for ephemeral gully incision, *Geomorphology*, 16, 161–173, 1996.
- 595 Vanmaercke, M., Poesen, J., Van Mele, B., Demuzere, M., Bruynseels, A., Golosov, V., Bezerra, J. F. R., Bolysov, S., Dvinskih, A., Frankl, A., Fuseina, Y., Guerra, A. J. T., Haregeweyn, N., Ionita, I., Makanzu Imwangana, F., Moeyersons, J., Moshe, I., Nazari Samani, A., Niacsu, L., Nyssen, J., Otsuki, Y., Radoane, M., Rysin, I., Ryzhov, Y. V., and Yermolaev, O.: How fast do gully headcuts retreat?, *Earth-Science Reviews*, 154, 336–355, <https://doi.org/10.1016/j.earscirev.2016.01.009>, 2016.



- Vannoppen, W., De Baets, S., Keeble, J., Dong, Y., and Poesen, J.: How do root and soil characteristics affect the erosion-reducing potential of plant species?, *Ecological Engineering*, 109, 186–195, <https://doi.org/10.1016/j.ecoleng.2017.08.001>, 2017.
- 600 Vanwalleghem, T., Poesen, J., Nachtergaele, J., Deckers, J., and Eeckhaut, M. V. D.: Reconstructing rainfall and land-use conditions leading to the development of old gullies, *The Holocene*, 15, 378–386, 2005.
- Verstraeten, G., Bazzoffi, P., Lajczak, A., Rădoane, M., Rey, F., Poesen, J., and De Vente, J.: Reservoir and Pond Sedimentation in Europe, *Soil Erosion in Europe*, pp. 757–774, <https://doi.org/10.1002/0470859202.ch54>, 2006.
- 605 Vinci, A., Brigante, R., Todisco, F., Mannocchi, F., and Radicioni, F.: Measuring rill erosion by laser scanning, *Catena*, 124, 97–108, 2015.
- Wang, R., Zhang, S., Pu, L., Yang, J., Yang, C., Chen, J., Guan, C., Wang, Q., Chen, D., Fu, B., and Sang, X.: Gully Erosion Mapping and Monitoring at Multiple Scales Based on Multi-Source Remote Sensing Data of the Sancha River Catchment, Northeast China, *ISPRS International Journal of Geo-Information*, 5, 200, <https://doi.org/10.3390/ijgi5110200>, 2016.
- Watson, D. and Lafen, J.: Soil Strength, Slope, and Rainfall Intensity Effects on Interrill Erosion, *Transactions of the ASAE*, 29, 0098–0102, 610 1986.
- Wei, R., Zeng, Q., Davies, T., Yuan, G., Wang, K., Xue, X., and Yin, Q.: Geohazard cascade and mechanism of large debris flows in Tianmo gully, SE Tibetan Plateau and implications to hazard monitoring, *Engineering Geology*, 233, 172–182, 2018.
- Wells, R. R., Momm, H. G., Rigby, J. R., Bennett, S. J., Bingner, R. L., and Dabney, S. M.: An empirical investigation of gully widening rates in upland concentrated flows, *Catena*, 101, 114–121, <https://doi.org/10.1016/j.catena.2012.10.004>, 2013.
- 615 Wischmeier, W. H. and Smith, D. D.: Predicting rainfall erosion losses - a guide to conservation planning, Tech. rep., USDA, Hyattsville, 1978.
- Woodward, D. E.: Method to predict cropland ephemeral gully erosion, *Catena*, 37, 393–399, 1999.
- Yao, C., Lei, T., Elliot, W. J., Mccool, D. K., Zhao, J., and Chen, S.: Critical Conditions for Rill Initiation, *Soil & Water Division of ASABE*, 51, 107–114, 2008.
- 620 Yibeltal, M., Tsunekawa, A., Haregeweyn, N., Adgo, E., Meshesha, D. T., Aklog, D., Masunaga, T., Tsubo, M., Billi, P., Vanmaercke, M., Ebabu, K., Dessie, M., Sultan, D., and Liyew, M.: Analysis of long-term gully dynamics in different agro-ecology settings, *Catena*, 179, 160–174, <https://doi.org/10.1016/j.catena.2019.04.013>, 2019.
- Zhang, S., Foerster, S., Medeiros, P., de Araújo, J. C., and Waske, B.: Effective water surface mapping in macrophyte-covered reservoirs in NE Brazil based on TerraSAR-X time series, *International Journal of Applied Earth Observation and Geoinformation*, 69, 41–55, 625 <https://doi.org/10.1016/j.jag.2018.02.014>, 2018.

# Physically-based model for gully simulation: application to the Brazilian Semiarid Region

Pedro Henrique Lima Alencar<sup>1,2</sup>, José Carlos de Araújo<sup>2</sup>, and Adunias dos Santos Teixeira<sup>2</sup>

<sup>1</sup>TU Berlin, Institut für Ökologie, 10587 Berlin, Germany

<sup>2</sup>Federal University of Ceará, Departamento de Engenharia Agrícola, Fortaleza, Brazil

**Correspondence:** Pedro Alencar (pedro.alencar@campus.tu-berlin.de); José Carlos de Araújo (jcaraujo@ufc.br)

**Abstract.** Gullies lead to land degradation and desertification, an increasing environmental and societal threat especially in arid and semiarid regions, despite of which there is a lack of research initiatives in this regard. As an effort to better understand soil loss in those systems, we studied small permanent gullies, a recurrent problem in the Brazilian North-eastern semiarid region. The increase of sediment connectivity and reduction of soil moisture, among other deleterious consequences, endangers this desertification-prone region and reduces its capacity to support life and economic activities. Hereafter, we propose a model to simulate gully-erosion dynamics, derived from the previous physically-based models by Foster and Lane and by Sidorchuk. The models were adapted so as to simulate long-term erosion. A threshold area shows the scale dependency of gully erosion internal processes (bed scouring and wall erosion). To validate the model, we used three gullies ageing over six decades in an agricultural basin in the State of Ceará. The geometry of the channels was assessed using UAV (Unmanned Aerial Vehicle) and Structure-from-Motion technique. Laboratory analyses to obtain soil properties were performed. Local and regional rainfall data were gauged to obtain sub-daily rainfall intensities. The threshold value (cross-section area of 2 m<sup>2</sup>) characterise when erosion in the walls due to loss of stability becomes more significant than sediment detachment in the wet perimeter. The 30-minute intensity can be used when no complete hydrographs from the rainfalls are available. Our model can satisfactorily simulate the gully-channel cross-section area growth over time, yielding Nash-Sutcliffe efficiency of 0.85 and  $R^2$  of 0.94.

15 *Copyright statement.*

## 1 Introduction

On our way to sustainable development and environmental conservation, soil erosion by water was pointed out as a key problem to be faced in the 21<sup>st</sup> century (Borrelli et al., 2017; Poesen, 2018). The impact of water-driven soil erosion, on the economy and food supply alone, represents an annual loss of US\$ 8 to 40 billion; a cut in food production of 33.7 million tonnes; an increase in water usage by 48 km<sup>3</sup>. These effects are felt more severely in countries like Brazil, China and India; and low-income households worldwide (Nkonya et al., 2016; Sartori et al., 2019). Estimates on total investments to mitigate land-degradation effects on site (e.g. productivity losses) and their off-site effects (e.g. biodiversity losses, water body siltation) lead to more

alarming values, averaging US\$ 400 billion yr<sup>-1</sup> (Nkonya et al., 2016). Nonetheless, those values were obtained by studies of soil loss using USLE (Universal Soil Loss Equation) or similar methods, none considering gully erosion. Thus, the real  
25 economical and social impacts of soil erosion are not completely comprehended as long as we do not understand better gully erosion and how to model it.

Gully erosion consists of a process that erodes one (or a system of) channel(s) that starts mainly due to the concentration of surface water discharge erosion during intense rainfall events (Bernard et al., 2010). The concentrated flow causes a deep topsoil incision and may reach the groundwater table and sustain the process (Starkel, 2011). Gully initiation is connected to  
30 anthropogenic landscape modifications and to land use and land cover changes, as observed in the other tropical biomes (Katz et al., 2014; Hunke et al., 2015; Poesen, 2018). On the other hand, the presence of vegetation may prevent soil erodibility both by increasing cohesion forces and enhancing soil structure (Vannoppen et al., 2017). Maetens et al. (2012) suggested that land-use changes lead to runoff changes and, hence, directly affect erosive processes. Gully erosion can also be affected by climate change, e.g., an increase of rainfall intensity could lead to higher erosive potential (Figueiredo et al., 2016; Panagos  
35 et al., 2017). Gullies are strongly dependent of landscape factors. With the advance of machine-learning techniques and the use of large data sets, some of the factors that mostly influence gully formation were identified, such as lithology, land use and slope. Some indexes were also pointed as relevant to indicate gully initiation, as the Normalized Difference Vegetation Index, Topography Wetness Index and Stream Power Index (Arabameri et al., 2019; Azareh et al., 2019).

Gullies play a relevant role in the connectivity of catchments (Verstraeten et al., 2006), allowing more sediment to reach  
40 water bodies and, thus, increasing siltation (de Araújo et al., 2006). For being particularly relevant among the erosion processes, gullies execute a great pressure on landscape development: they change the water-table height, alter sediment dynamics and increase runoff (Valentin et al., 2005; Poesen, 2018; Yibeltal et al., 2019). They represent an increasing risk to society and environment for affecting land productivity, water supply, floods, debris flow and landslides (Liu et al., 2016; Wei et al., 2018). Gullies also have a large impact on economy due to high mitigation costs, a reduction of arable fields, a decrease of  
45 groundwater storage, an increase of water and sediment connectivity and more intense reservoir siltation (Verstraeten et al., 2006; Pinheiro et al., 2016). The assessment of gully impacts on production costs in an arid region of Israel showed that costs of gully mitigation represent over 5% of total investments, and production losses are as large as 37 % (Valentin et al., 2005).

The State of Ceará, located in the semiarid region, has its total area (over 148000 km<sup>2</sup>) included in the risk zone of desertifi-  
50 cation. From this total, about 11.5% is also under advanced land degradation conditions, including the formation of Badlands and Gullies, a similar condition to the one found in other desertification hotspots in the semiarid (Mutti et al., 2020). The region is also especially vulnerable to climate change (Gaiser et al., 2003), and both degradation and desertification can be accelerated by gullies (Zweig et al., 2018). The Brazilian semiarid region is also characterised by shallow crystalline rock bed that with scarce groundwater and baseflow, which makes the its population rely almost exclusively in superficial reservoirs for water supply (Coelho et al., 2017). Therefore, gullies are a two-way threat, first by depleting the already scarce groundwater  
55 and second by increasing sediment connectivity, causing siltation and resulting in loss of storage capacity and water quality (Verstraeten et al., 2006).

Despite their relevance to hydro-sedimentological processes, gullies are often neglected in models (Poesen, 2018), and should be directly addressed (Paton et al., 2019). However, gully erosion is a process with the interaction of many variables, many of them difficult to assess (Bernard et al., 2010; Castillo and Gómez, 2016): according to Bennett and Wells (2019),  
60 for instance, no model has ever been presented to clearly explain the process of gully formation. Among the models that do consider gully erosion, the use of empirical approach prevails (e.g. Thompson (1964); Woodward (1999); Nachtergaele et al. (2002); Wells et al. (2013)); whereas others focus primarily on physically-based algorithms (e.g. Foster and Lane (1983); Hairsine and Rose (1992); Sidorchuk (1999); Dabney et al. (2015)).

It is, therefore, an important milestone to understand how gully erosion starts and develops (Poesen, 2018). The objective of  
65 this work is to propose a physically-based model that predicts growing dynamics and sediment production in small permanent gullies in a hillslope scale. In order to achieve this, we tested two models – Foster and Lane (1983) and Sidorchuk (1999) – and two adapted models, being one modification of the model of Foster and Lane and the other the coupling of both models. To validate the model, we selected three small permanent gullies in the State of Ceará. The gullies geometry was assessed using UAV (Unmanned Aerial Vehicle) and the soils were sampled and characterised.

70 We understand by small permanent gullies as the result of active erosive processes that form channels by concentrated flow and do not interact with groundwater. Normally, these gullies could be remedied by regular tillage process, but in abandoned or unclaimed land they usually remain untreated for long periods. Although the land where they develop is usually unused for economic activities besides livestock grazing in open range, the development of such gullies threatens the ecosystem and community.

## 75 2 MATERIALS AND METHODS

### 2.1 Study area

The Brazilian Semiarid Region (1 million km<sup>2</sup>) is covered mainly by the Caatinga biome with vegetation characterised by bushes and broadleaf deciduous trees (Pinheiro et al., 2013). The region is prone to droughts and highly vulnerable to water scarcity (Coelho et al., 2017). More than 25 million people live in this region, where agriculture (maize, beans, cotton) and  
80 livestock in open range are of utmost socio-economic relevance. Usually, rural communities use deleterious practices, such as harrowing and field burning, which enhance the risk of intense erosive processes. These characteristics lead to a scenario of soil erosion and water scarcity with high social, economic and environmental consequences (Sena et al., 2014). Erosion in general (and gullies in particular) increases local water supply vulnerability due to reservoir siltation (de Araújo et al., 2006) and water-quality depletion (Coelho et al., 2017).

85 The study area is located in the Madalena Representative Basin (MRB, 75 km<sup>2</sup>, state of Ceará, north-eastern Brazil; see Figure 1), inserted in the Caatinga biome, a dry environment with a semiarid hot BSh climate, according to the Köppen classification. The annual precipitation averages 600 mm, concentrated between January and June (Figure 2); and the potential evapotranspiration totals 2,500 mm yr<sup>-1</sup>. Geologically, the basin is located on top of the crystalline bedrock with shallow soils and limited water storage capacity. The rivers are intermittent and runoff is low, typically ranging from 40 to 60 mm yr<sup>-1</sup>

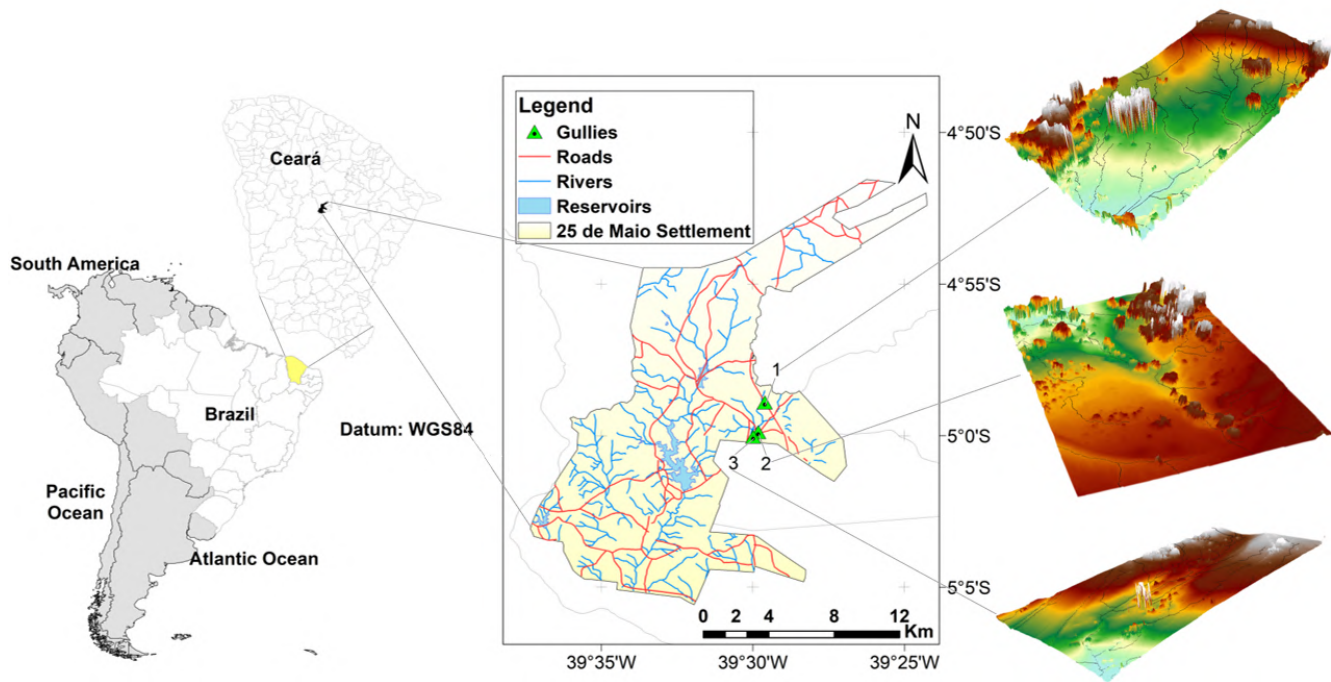


**Figure 1.** Location of the study area and the gully sites (gullies 1, 2 and 3) and the digital elevation models. The roads, rivers and reservoirs were mapped by Silva et al. (2015).

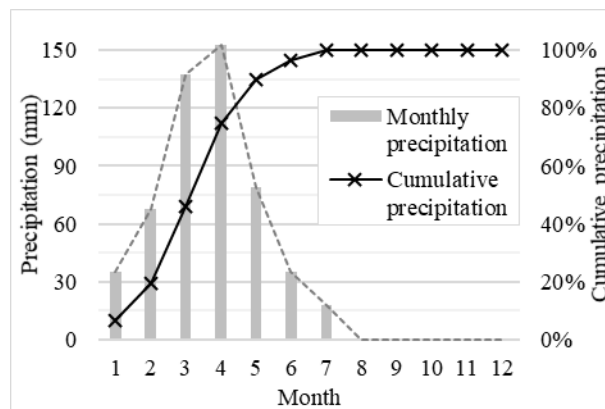


**Figure 2.** Monthly precipitation (median) and cumulative precipitation at MRB from 1958 to 2015.

90 (Gaiser et al., 2003). The basin is located within a land reform settlement with 20 inhabitants per km<sup>2</sup>, whose main economic activities are agriculture (specially maize), livestock and fishing (Coelho et al., 2017; Zhang et al., 2018).

Three gullies were selected for this study, all located on the eastern portion of the basin. The studied gullies have the following dimensions (average ± standard deviation): projection area (317±165 m<sup>2</sup>), length (38 ± 6 m), volume (42 ± 25 m<sup>3</sup>),



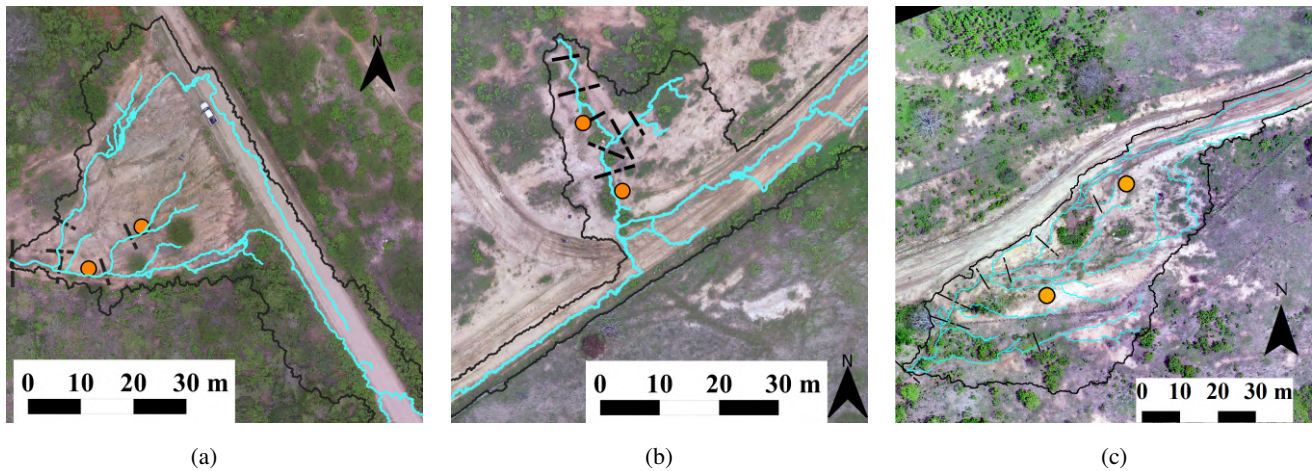


**Figure 3.** Aerial photogrammetry of the studied gullies. Note that they are at the margin of the road, receiving the concentrated flow diverged from it. The continuous black line represents the catchment boundaries; the blue line represents the flow paths; the dashed black lines are the cross-sections used on the validation of the model and; the orange dots are the soil sampling points - (a) gully 1; (b) gully 2; (c) gully 3.

**Table 1.** Coordinates of the three gullies used in this study (Datum: WGS84).

Area	Latitude	Longitude
Gully 1	04°58'54.3"S	39°29'36.4"W
Gully 2	04°59'53.1"S	39°29'49.4"W
Gully 3	05°00'02.4"S	39°29'59.4"W

depth ( $0.44 \pm 0.25$  m) and eroded mass ( $61 \pm 36$  Mg). The coordinates are presented in Table 1. Despite their small sizes, they possess a significant impact on the landscape for reducing productive areas and soil fertility. According to the information obtained from local villagers, gully erosion started immediately after the construction of a country road in 1958 (Figure 3). Before the construction, the sites were covered by Caatinga vegetation (Pinheiro et al., 2013). The road modified the natural drainage system and does not provide for any side nor outlet ditches, therefore generating a concentrated runoff at its side. This has caused excessive runoff on the hillslopes and triggered gully erosion.

## 100 2.2 Topography survey

The assessment of the gully data was achieved using an Unmanned Aerial Vehicle (UAV), a technique applied in other regions as well (Stöcker et al., 2015; Wang et al., 2016; Agüera-Vega et al., 2017). A UAV equipped with a 16 MP camera (4000 x 4000 pixels) and view field of 94 % was used. The flight was at 50 m altitude with a frontal overlap of 80 % and lateral overlap of 60 %. For the geo-reference of the mosaic, five ground control points were deployed, which were evenly distributed in each area, both in high and low ground. The coordinates were collected using a stationary GNSS – RTK (L1/L2) system with centimetre-level accuracy. The Digital Surface Model was produced using the Structure from Motion technique. The process consists of a



three-dimensional reconstruction of the surface, derived from images and the generation of a dense cloud of 3D points based on the matching pixels of different pictures and Ground Control Points (GPCs); the processing result is a model as accurate as one obtained by laser surveys (e.g., Light detection and ranging - LiDAR), but cheaper and less time consuming (Stöcker et al., 2015; Agüera-Vega et al., 2017). The ground sample distance (pixel size) obtained is of four to five centimetres and the digital models have high precision, with a vertical position error of one centimetre and horizontal error of six millimetres. The vegetation, yet sparse, was an obstacle to increasing the quality of the survey. However, as the focus of this study was the gully cross-section geometry, vegetation interference was acceptably low.

### 2.3 Soil data

Due to the scale of this experiment and the homogeneity of the soil-vegetation components (Güntner and Bronstert, 2004) we divided the areas in two sets based on grain-size distribution, organic matter and bulk density. Gully 1 (G1) has specific features and comprises the first soil (S1), whereas gullies G2 and G3, close to each other, are represented by the second soil (S2).

At the gully sites, soil surveys were carried out to assess the properties and parameters required to implement the model: undisturbed soil samples were collected (see Figure 3) at depths of 0.10 m, 0.30 m and 0.50 m (two sites, three depths, three samples per depth, totalling 18 samples collected). At the depth of 0.50 m, a well-defined horizon C, rich in rocks and soil under formation, was identified. The maximum depth of the non-erodible layer ranged from 60 to 75 cm in all gullies. We performed grain-size distribution, sedimentation, organic matter, bulk density and particle density analysis.

The soils are loamy, with clay content ranging from 6 % to 37 %. The particle density is  $2580 \text{ kg m}^{-3}$ . The soils are Luvisols and have typical profile, with the top layer relatively poor in clay when compared to the layers below and with the regular occurrence of gravel at the surface. Furthermore, Luvisols are rich in active clay, which makes them prone to form cracks and macropores when dry (dos Santos et al., 2016), a process also documented in soils with similar texture in a semiarid area in Spain (van Schaik et al., 2014). Rill erodibility values ( $K_r$ ) and critical shear stress ( $\tau_c$ ) for the soils were obtained using the Equations 1 and 2 (Alberts et al., 1995) and are also presented in Table 2.

$$K_r = 0.00197 + 0.00030\%VFS + 0.038633e^{(-1.84\%OM)} \quad (1)$$

$$\tau_c = 2.67 + 0.065\%C - 0.058\%VFS \quad (2)$$

where  $\%VFS$  is the percentage of very fine sand,  $\%C$  is the percentage of clay and  $\%OM$  is the percentage of organic matter.

### 2.4 Rainfall data

Daily rainfall data for the location covering the entire period was provided by the Foundation of Meteorology and Water Resources of Cear  (Funceme). We used five rain-gauge stations in the region, covering the period from 1958 to 2015. The double mass method was employed to check data consistency (Supplementary material - Fig. S1). The gaps in the measurements

**Table 2.** Grain-size distribution, organic matter for both soils (S1 - for the gully 1 - and S2 - for the gullies 2 and 3) at three depths (10, 30 and 50 centimetres) and the respective texture classification (USDA); and the estimated (in italic) rill erodibility ( $K_r$ ) and critical shear stress ( $\tau_c$  of the site soils) obtained using Equations 1 and 2.

Soil and layer	Gravel > 2 mm	FCS <sup>a</sup> > 0.1 mm	VFS <sup>b</sup> > 0.05 mm	Silt > 0.002 mm	Clay < 0.002 mm	Organic Matter	Bulk density (kg m <sup>-3</sup> )	Soil Class	$K_r$ (s.m <sup>-1</sup> )	$\tau_c$ (Pa)
S1-10	13 %	45 %	21 %	11 %	10 %	3.1 %	1699	Sandy Loam	<i>0.015</i>	<i>2.102</i>
S1-30	6 %	46 %	16 %	14 %	18 %	3.3 %	1677	Sandy Loam	<i>0.016</i>	<i>2.912</i>
S1-50	4 %	63 %	20 %	7 %	6 %	2.2 %	1765	Loamy Sand	<i>0.020</i>	<i>1.900</i>
S2-10	17 %	33 %	22 %	11 %	17 %	4.9 %	1509	Sandy Loam	<i>0.012</i>	<i>2.499</i>
S2-30	8 %	29 %	6 %	20 %	37 %	5.7 %	1572	Clay Loam	<i>0.011</i>	<i>4.611</i>
S2-50	2 %	28 %	15 %	20 %	25 %	1.4 %	1643	Loam	<i>0.014</i>	<i>3.425</i>

<sup>a</sup> Fine to Coarse Sand; <sup>b</sup> Very Fine Sand.

(January 1958 and September 1960) were filled by the nearest gauging station. The annual rainfall in the area averages 613 mm (Supplementary material - Fig. S2) with coefficient of variation of 43%, typical values for the Brazilian Semiarid Region (de Araújo and Piedra, 2009).

140 The modelling of the gullies is based on peak discharge, which demands sub-daily rainfall data, but only daily precipitation is available inside the study basin covering the whole experiment period. To proceed with the modelling, correlation curves relating total daily precipitation and rainfall intensity were used. In order to define which was the best intensity to be used in the modelling, four were tested (Figure 4) as input for the model: average ( $I_{av}$ ), sixty-minute maximum ( $I_{60}$ ), thirty-minute maximum ( $I_{30}$ ) and fifteen-minute maximum ( $I_{15}$ ) intensities.

145 To build such curves we used, data from the Aiuaba Experimental Basin's (AEB) detailed hydrographs, which have been monitored since 2005 (Figueiredo et al., 2016). This experimental basin is located 190 km south of MRB and both basins are climatically homogeneous (Mendes, 2010). In addition, in Figure 4 shows the rainfall data for the MRB collected during the rainy season in 2019 (January to July). We can observe that the data has similar behaviour but constantly on the lower area of the plot. It is relevant to note that the year of 2019 in MRB was dry and such behaviour is expected.

150 To obtain discharge values from intensity we used the SCS-CN method (Chow, 1959). For the models, the main rainfall-related variables are the event peak discharge and its respective duration. Because the gully catchment areas are very small, their respective concentration time is negligible compared with the intense-rainfall duration in the region (Figueiredo et al., 2016), yielding a uniform pattern of peak discharge.

## 2.5 Gully modelling

155 To model small permanent gullies we propose two models based in classical formulations from the literature - Foster and Lane (1983) and Sidorchuk (1999). The Foster and Lane Model (FLM) is one of the most used models of gully erosion, based on net shear stress and transport capacity. The FLM assumes a rectangular cross-section and was originally designed for single-

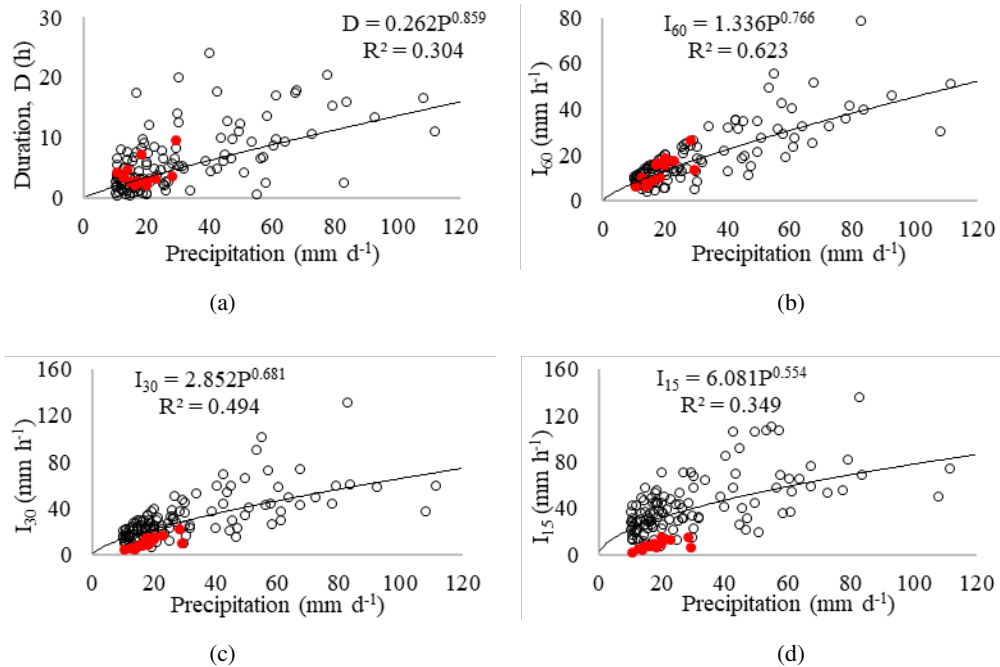


**Figure 4.** Correlation between daily precipitation and sub-daily variables at the Aiuaba Experimental Basin (Figueiredo et al., 2016). (a) daily precipitation versus event duration ( $D$ ); (b) daily precipitation versus 60-minute maximum intensity ( $I_{60}$ ); (c) daily precipitation versus 30-minute maximum intensity ( $I_{30}$ ); and (d) daily precipitation versus 15-minute maximum intensity ( $I_{15}$ ). The white circles indicate data obtained in Aiuaba from 2005 to 2014. The red dots indicate precipitations measured in the MRB from January to July 2019 (rainy season).

rainfall ephemeral gully modelling. The Sidorchuk Model (SM) takes considers mass balance of sediment, shear stress (in terms of critical velocity), soil cohesion and the Manning equation to estimate the cross-section geometry and channel slope. It also uses empirical equations based on field measurement to estimate the flow depth and width. The model gives special attention to the processes involving gully wall transformation. A description of both models is available in the literature and in the supplement materials of this paper.

The proposed models are the Adapted Foster and Lane Model (FLM- $\lambda$ ) and the coupled model Foster and Lane & Sidorchuk Model (FL-SM). The key difference between the two proposed models is the amount of data required to use each one. The models are presented below.

### 2.5.1 Adapted Foster and Lane Model (FLM- $\lambda$ )

The Foster and Lane Model (FLM), as proposed by its authors, considers a single source of erosion: The soil detached from the channels bed and walls due to shear stress. Based on field observation and literature (Blong and Veness, 1982), however, show that wall instability and failure can represent a significant source of sediment. To estimate the effect of wall erosion at the studied site, we proposed an empirical parameter ( $\lambda$  – Eq. 3) to correct the effect of lateral flow and wall erosion. This multiplicative parameter was calibrated and validated as function of the catchment shape, based on two coefficients: the

Gravelius coefficient ( $K_G$  – Eq. 4) and the Form coefficient ( $K_F$  – Eq. 5). Both coefficients describe the geometry of the catchment area and can be interpreted as how compact the distribution of area is. Commonly linked to flood proneness, these parameters also relate to the transversal distance of the catchment area, which influences the amount of lateral inflow into the mainstream.

$$\lambda = \frac{A_o}{A_m} \quad (3)$$

$$K_G = 0.28 \cdot \frac{C_P}{C_A} \quad (4)$$

$$K_F = \frac{C_A}{C_L^2} \quad (5)$$

In Equation 3 the terms  $A_o$  and  $A_m$  are the observed and measured cross-section area and in Equations 4 and 5,  $C_P$ ,  $C_A$  and  $C_L$  stand for the catchment perimeter, area and length, respectively.

The plot of  $\lambda$  versus both parameters are presented in Figure 5. Two equations [ $\lambda(K_G)$  and  $\lambda(K_F)$ ], see Figure 5] were calibrated using data from 14 randomly selected sections out of the 21 assessed by the DEM. The remaining data were used to validate the equations. The model FLM- $\lambda$  consists on processing the FLM as originally proposed and, afterwards, multiplying the output area by the  $\lambda$  correction parameter. Thus increasing proportionally the total area, as a proxy to wall erosion processing.

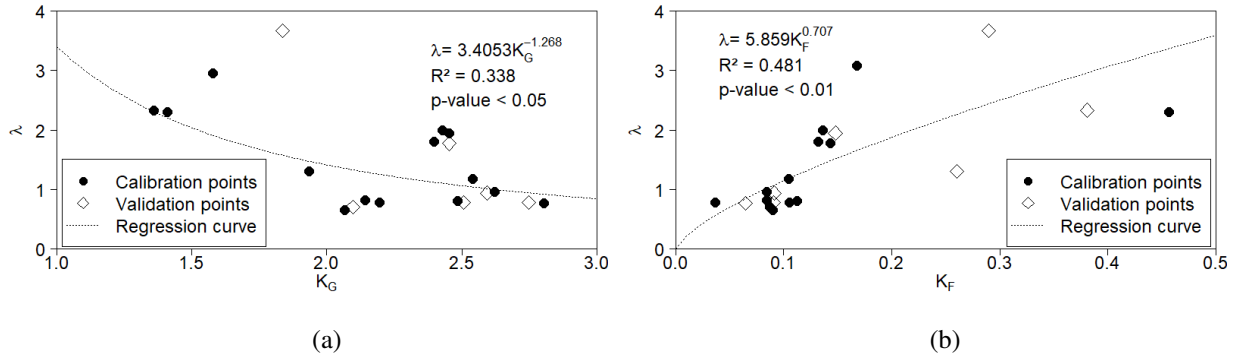


**Figure 5.** Correlations between the ratio ( $\lambda = A_o/A_m$ ) and (a) the Gravelius coefficient ( $K_G$ ) and (b) the form factor ( $K_F$ ) for 21 monitored cross-sections at MRB. Black dots refer to calibration cross-sections and white diamonds refer to validation cross-sections. The values of  $R^2$  indicated in the plots are for the calibration. The validation  $R^2$  were 0.10 for  $K_G$  and 0.54 for  $K_F$ .

$$\lambda = \max(5.859K_F^{0.707}; 1.0) \quad (6)$$

The coefficient ( $K_F$ ) yielded a positive Nash-Sutcliffe Efficiency value and smaller RMSE (0.17 and 0.67 respectively), which did not occur with the Gravelius coefficient (-2.43 and 0.84 respectively). In the revised model, hereafter addressed as FLM- $\lambda$ , the FLM area output is multiplied by the calibrated parameter  $\lambda$  (Equation 6), yielding the eroded area. Applying this factor caused a significant improvement in model efficiency, with NSE increasing from 0.557 to 0.757. The incremental area produced by the multiplication of  $\lambda$  is assumed to increase the width of the upper half of the cross-section, keeping bottom width and the orthogonality of the walls unchanged.

### 2.5.2 Coupled Model – Foster and Lane & Sidorchuk Model (FL-SM)

The previous model was produced due to the necessity of considering wall failure as a sediment source and used an empirical approach. Another, using a physically-based concept, is to include the specific routine of the Sidorchuk model that tackles wall failure in the Foster and Lane model. This can be achieved by simply including a test after each event, checking if the depth of the channel causes wall instability given the current angle of the bank.

By analysing the data, however, we identified that for small cross-sections, even after the critical had been reached, the section remained rectangular. This implies an additional threshold mechanism related to the geometry of the channel and/or catchment. Therefore, the FL-SM requires the determination of a threshold value for the implementation of the wall erosion equations. Such a threshold controls when the wall erosion becomes significant for the total amount of eroded soil. In the model, it represents the limit stage, above which Sidorchuk (1999) equations are used. It also represents the scale when solely the channel bed erosion, described by the Foster and Lane (1983) equations start to consistently underestimate the measured area. In this study we used the Foster and Lane model to identify this scale where the both processes (channel bed and wall erosion) switch relevance.

A flow chart of the FL-SM is presented below. The core of the model is the Foster and Lane Model, processed for every runoff event. When the cross-section reaches the threshold condition and satisfies the criteria for wall failure as described in Sidorchuk (1999) a new step is included, that calculates wall transformation.

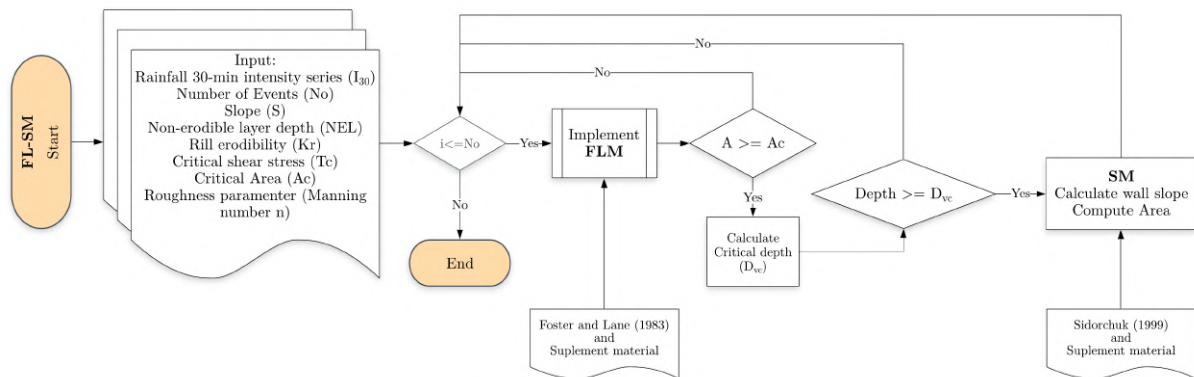


Figure 6. Flow chart of the Coupled model FL-SM.

## 2.6 Model fitness evaluators

210 To assess the goodness-of-fit, the Nash-Sutcliffe Efficiency coefficient (NSE); the root mean square error (RMSE); and the percent bias (PBIAS) were used (see Moriasi et al. (2007)). Besides, the methodology proposed by Ritter and Muñoz-Carpena (2013) asserts statistical significance to the evaluators. The proposed model is based on Monte Carlo sample techniques to reduce subjectivity when assessing the goodness-of-fit of models.

$$NSE = 1 - \frac{\sum_{i=1}^n (X_{o,i} - X_{m,i})^2}{\sum_{i=1}^n (\bar{X}_o - X_{o,i})^2} \quad (7)$$

$$215 \quad RMSE = \sqrt{\frac{\sum_{i=1}^n (X_{o,i} - X_{m,i})^2}{n}} \quad (8)$$

$$PBIAS = \frac{\sum_{i=1}^n (X_{o,i} - X_{m,i})}{\sum_{i=1}^n (X_{o,i})} \quad (9)$$

In Equations 7, 8 and 9,  $X_{o,i}$  is an observation and  $X_{m,i}$  a modelled value, being  $n$  the total of observations and simulations.  $\bar{X}_o$  is the average of the observed values.

## 3 RESULTS

### 220 3.1 Gully modelling

From the three gullies measured, twenty-one cross-sections with different dimensions were selected and used to validate and compare the models quality. Figure 7 presents the scatter of modelled and measured data for the models implemented. The FL-SM presented a Nash-Sutcliffe Efficiency coefficient of 0.846 when using a threshold for the area of the cross-section of 2.2 m<sup>2</sup>. In Figure 8 some output examples for the sections above the threshold are presented.

225 In terms of geometry, sections below the threshold have cross-sections similar to Figure 8 [(a), (b), (c)], with rectangular-like shape, unless the  $\lambda$  parameter is reintroduced, which leads to cross-sections like Figure 8 [(d), (e), (f)], with piled rectangles. When the area surpasses the threshold value, sections have mainly trapezoidal geometry, as illustrated in Figure 8 [(g), (h), (i)]. It is important to highlight that the model can produce triangular geometry, but none was obtained in this study.

#### 3.1.1 Threshold analysis

230 The interpretation of the threshold for implementation of the wall erosion routine can be based on (a) the cross-section area or (b) the catchment geometry, as illustrated in Figure 9. The first approach considers a critical area that once reached marks when the wall erosion is really significant over the other processes. In this study the threshold identified was at an area of 2.2

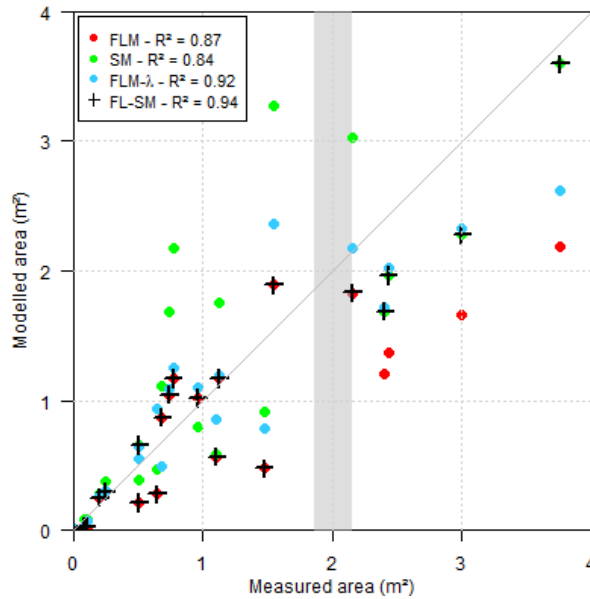


**Figure 7.** Performance of the coupled model (FL-SM), Foster and Lane Model (FLM and FLM- $\lambda$ ) and the Sidorchuk model (SM). P-value  $< 0.001$  for all sets. The grey bar indicates the identified area threshold where there is a change and SM becomes consistently better than the FLM.

$m^2$ . After that, the model calculates the effect of sidewall erosion and reaches the critical final area for the analysed section. The presence of a threshold for applying the sidewall erosion routine indicates a change of relevance among processes on a given scale. Although the threshold is addressed as an area, this is only a consequence of more complex interactions among discharge, flow erosivity, cohesion and gravitational forces.

The second interpretation is related to the catchment geometry, as the approach given to the parameter  $\lambda$  also related to the  $K_F$ . From the distribution of the cross-sections we can observe sections that are better modelled by SM even under the threshold. By analysing the values of form coefficient ( $K_F$ ) of each set (Figure 9b) we observed that set 1 has  $K_F$  of  $(0.08 \pm 0.02)$  and set 2 has  $0.22 (\pm 0.12)$ . Higher values of  $K_F$  indicate a more compact catchment, with more lateral flux into the channel, therefore producing more erosion in the soil. By sorting the model results of FLM and SM based in the form coefficient, using the threshold of  $K_F = 0.15$ , we obtained an NSE of 0.79.

Given the obtained efficiencies, in this study we adopted a threshold based on the cross-section area, however the use of a catchment-based threshold should not be discarded and could be promising, once in the literature are evidenced of the relation between lateral flow and gully erosion (Blong and Veness, 1982).



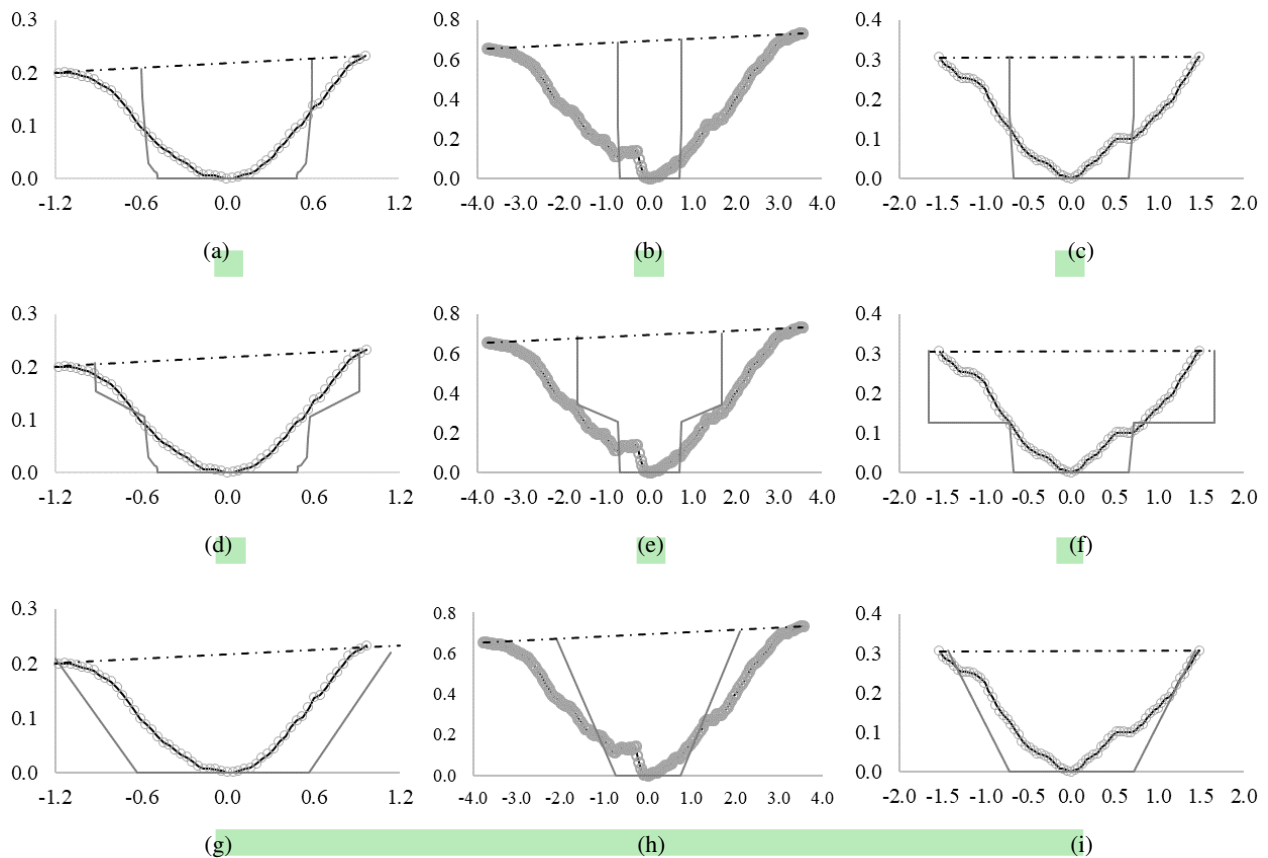


**Figure 8.** Some examples of gully cross-sections measured (black line with circles) and the modelled (dark grey line) geometry. figures (a), (b) and (c) show the output for the model of Foster and Lane; figures (d), (e) and (f) the output for the model of Foster and Lane adapted with the parameter  $\lambda$  and figures (g), (h) and (i) the result from the Sidorchuk Model (SM). Distances in metres. Section in (a, d and g) is a section obtained from gully 1, (b, e and h) from gully 2, and (c, f and i) from gully 3.

### 3.1.2 Rainfall intensity

From the three gullies, twenty-one cross-sections with no interference of bushes or trees were selected from the Digital Elevation Model. The FLM was tested for the 60-minute, 30-minute, 15-minute and average intensities [FLM( $I_{60}$ ), FLM( $I_{30}$ ), FLM( $I_{15}$ ), FLM( $I_{av}$ )]. It showed the best response when using the thirty-minute intensity [FLM( $I_{30}$ ); NSE = 0.557]. Figure 10 presents the plot of the model outputs for area compared with measured data. Moreover, the Foster and Lane Model did not show good responses to the cross-section geometry, regardless of the intensity tested. This may indicate a flaw of the model concerning the side-ward erosive process.

The FLM considers rectangular shaped cross-sections, but the field survey showed that the sections are rather trapezoidal or triangularly shaped (Figure 8). Among the factors that can shape gully walls, there are seepage, slope material, and the slope angle itself (Sidorchuk, 1999; Bingner et al., 2016). Besides, gully walls can be shaped by lateral discharge (Blong and Veness,

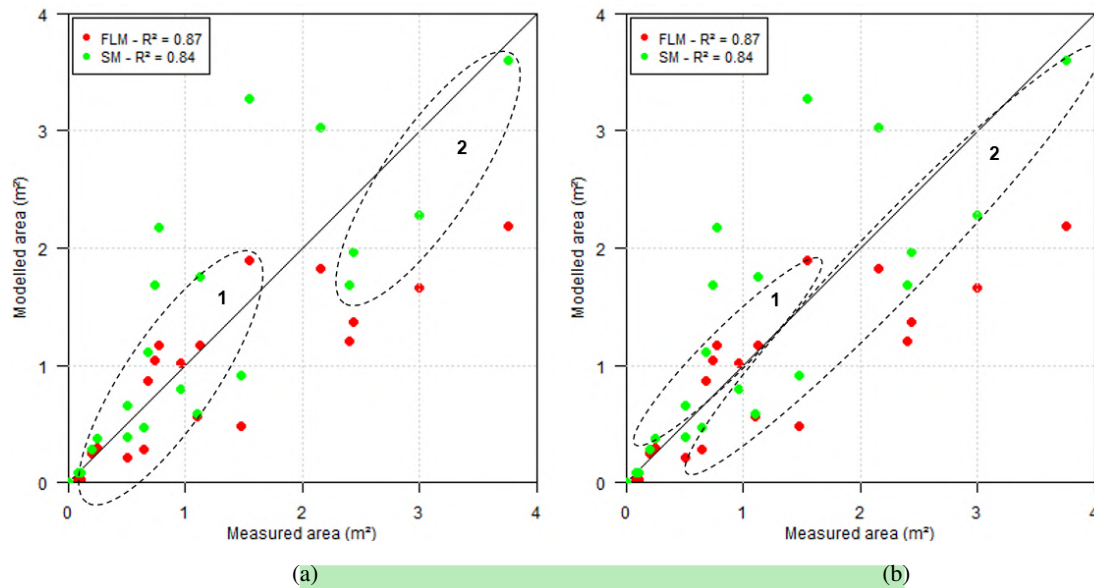


**Figure 9.** Thresholds for wall erosion: (a) based on the cross-section area; (b) based on the catchment geometry and  $K_F$ . In both plots the set 1 indicates the domain of bed erosion and Foster and Lane equations and set 2 the domain of wall erosion and Sidorchuk equations. p-value < 0.001.

1982), which depends directly on the morphology of the cross-section catchment area. Figure 10 also shows a tendency of the model in underestimating the cross-section area, which implies that the model does not consider all the relevant erosive processes. The sidewall erosion has proven to be a relevant source material, often representing over 50 % of the eroded mass (Crouch, 1987), whereas the FLM only assumes the vertical sidewall morphology. Therefore, in this study we adopted the 30-minute intensity as the standard intensity and duration to assess peak-discharge.

### 3.2 Model evaluators

The coupled model, FL-SM, presented the highest performance of goodness-of-fit evaluators (Figure 11). The model yielded a PBIAS value below 10 %, which is very good. The coupled-model RMSE was also low (0.397), whereas the NSE reached a value of 0.846, being classified as good (Ritter and Muñoz-Carpena, 2013) or very good (Moriassi et al., 2007).

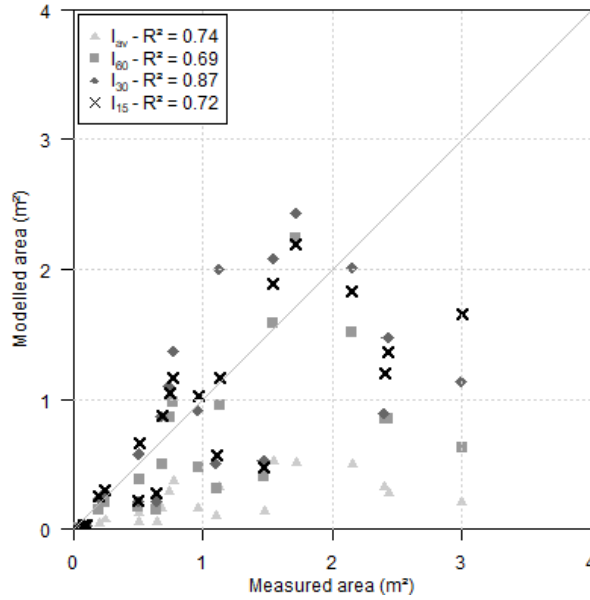


**Figure 10.** Results of the FLM for cross-section area using different intensities ( $I_{av}$  – average;  $I_{60}$  – 60-min;  $I_{30}$  – 30-min; and  $I_{15}$  – 15-min) to generate the peak discharge.

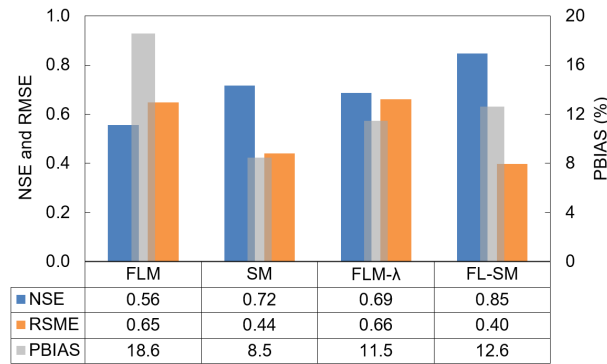


**Figure 11.** Model evaluators  $NSE$ ,  $RMSE$  and  $PBIAS$ . The bar plot shows the performance of all tested models – values of  $PBIAS$  in percentage.

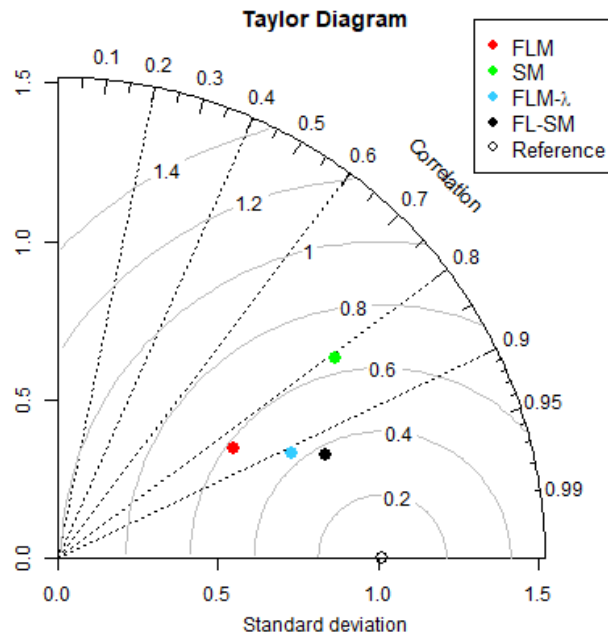


**Figure 12.** Taylor diagram for the model performance. The azimuthal distance gives the correlation ( $R$  - Pearson), the distance to the origin is proportional to the standard deviation of the model values and the distance to the Reference (measured data) is proportional to the  $RMSE$ .

265 Figure 11 shows the evolution of NSE values with more details so that conclusions can be drawn. The Foster and Lane model with  $\lambda$  parameter (FLM- $\lambda$ ) was calibrated with 14 cross-sections out of 21 and performed as well as the Sidorchuk model (SM), which considers the sidewall effect. For the coupled model, there is no efficiency gain when applying the calibrated parameter ( $\lambda$ ) to sections below threshold which indicates that the lateral inflow is only relevant for larger sections. Figure 12 presents the Taylor diagram for comparison of the four models. In this diagram, the closer a model is from the reference (measured data) the better. The FL-SM presented the highest correlation and the lowest RMSE.

270 Another approach to estimate the goodness-of-fit of a model was proposed by Ritter and Muñoz-Carpena (2013). The routine (FITEVAL) consists of repeatedly re-sampling from the dataset and handles each re-sample as an actual sample of the population. This grants the generation of a confidence interval for statistical evaluators. The method classifies the model as acceptable to very good –  $NSE \in [0.66;0.95]$  for a p-value of 0.05. A conservative interpretation of this result implies considering the lowest values as the minimum state of information, or as the one that contains (almost) no unproven hypothesis. As a consequence, and according to Ritter and Muñoz-Carpena (2013), the FL-SM can be classified as acceptable to very good. The detailed output of the FITEVAL analysis can be found in the supplementary material (Fig. S6).

### 3.3 Gully growing modelling

280 Gully growth is commonly described as being a fast process in the first years that, progressively slows down its enlargement. In our model, the mechanism that produces this dynamic is event piling. It could be observed that, after a particularly intense

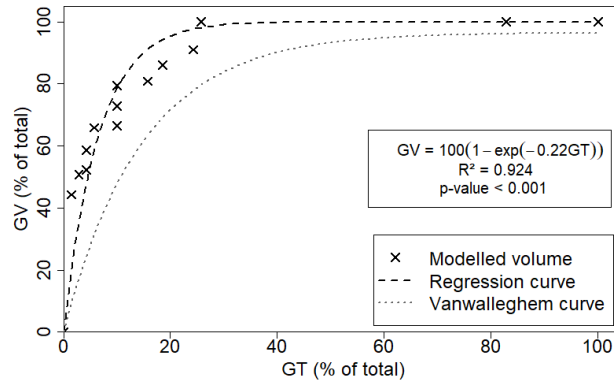


**Figure 13.** Behaviour of gully growing rate as proposed by literature (Vanwallegem et al., 2005; Poesen et al., 2006) and modelled (data from Gully 1).  $GV$  is the gully volume in percent and  $GT$  the gully age in percent

event, the channel is sufficiently wide, therefore, following less intense events produce only shallow flow and low shear stress, hence producing fewer or no sediment. Only when a more intense event than the last erosive one happens, there is further erosion. Our model mimics this growing dynamic and its periods between extreme events. Such behaviour is widely explored in the literature (Vanwallegem et al., 2005; Poesen et al., 2006; Poesen, 2018) and illustrated in Fig. 13. Vanwallegem et al. (2005), using several data-sets from previous studies found a strong correlation between  $GT$  (the percentage of the gully age over the total) and  $GV$  (the percentage of the gully volume over the total), given by a function as expressed in Eq. 10. The parameters  $\alpha$  and  $\beta$  were calibrated by Vanwallegem et al. (2005) as 96.5 and -0.07 with coefficient of determination ( $R^2$ ) equal to 0.99.

$$GV = \alpha[1 - \exp(\beta GT)] \quad (10)$$

The parameters  $\alpha$  (equals to 100) and  $\beta$  (equals to -0.22) obtained in our study differ from the values in the literature. While  $\alpha$  difference is due to a numerical formulation ( $GV_{total}$  is equal to the measured volume), the parameter  $\beta$  brings us some insights. Its absolute value for our data set is three times bigger than calibrated by Vanwallegem et al.. A larger  $|\beta|$  indicates a fast initial growth, possibly caused by the intensive rainfall regime of the region, with convective intense events and high erosivity (Medeiros and Araújo, 2014), a different condition from Belgium and Russia, where most studies that lead to Vanwallegem et al.'s equation were carried on. Therefore, although gully growth behaviour is similar in different regions, local conditions such as climate and land use should be taken into account.

### 3.4 Landscape development impacts on gully erosion

Gullies are scale-dependent phenomena and frequently related to thresholds due to their initiation, which is based on catchment area and slope (Torri and Poesen, 2014; Poesen, 2018). Both characteristics are directly linked to shear stress and stream power

300 when using physical gully models. Montgomery and Dietrich (1992) argue that changes in landscape and the drainage system can lead to a larger occurrence of channelization and its impacts can be noticed faster. Torri and Poesen (2014) suggest a threshold for head development in gullies as conveyed in Equation 11.

$$S C_A^{0.38} > k \quad (11)$$

where  $S$  ( $\text{m m}^{-1}$ ) is the slope,  $C_A$  (ha) is the catchment area and  $k$  is a parameter for channel and gully initiation.

305 For croplands in tropical conditions, the proposed value of  $k$  is 0.042 (Torri and Poesen, 2014). For the areas in the present study, we have channel initiation for values lower than half ( $k = 0.020$ ) and systematically lower than the field data of (Vandaele et al., 1996) could be observed. These findings suggest vulnerability of the region. Considering that the three experimental sites were located next to a road, this disturbance triggered gully initiation and other actions may cause similar problems in the region, such as deforestation and forest fire. The road not only enlarged the total catchment area, it also increased its length.

310 While relations between catchment length and area are well-established ( $L = b c_A^{0.49}$ ) with values of  $b$  varying from 1.78 to 2.02 (Montgomery and Dietrich, 1992; Sassolas-Serrayet et al., 2018), the present experiments found  $b$  equalling 3.17. With a smoother surface and almost no meandering, road construction caused modifications that promoted more energetic flows on the gully head. Road construction has also been identified as potential factor for gully initiation in other areas of the Brazilian Semiarid Region, as in the Salitre Catchment, where large gullies started after construction of an unpaved rural road (da Silva and Rios, 2018).

## 4 DISCUSSION

### 4.1 Model limitations

The proposed models, specially the FL-SM presented a significant improvement, reaching an efficiency over 0.8. Yet, some reflections can be made to understand when the models fail, as well as understand where new advances can be pursued.

#### 320 4.1.1 Foster and Lane Model (FLM)

The first attempt for this study was to identify which was the best peak and duration of rainfall to be considered. Due to the timescale of this work, it was required to select a single parameter for all the events. Therefore, a relevant result from this work is the confirmation that the 30-minute intensity is the one that provides most information about gully erosion. Wischmeier and Smith (1978) proposed the product of total storm energy and the 30-minute intensity to “predict the long-time average soil loss in runoff”. The use of  $I_{30}$  for estimating event-related gully erosion was previously experimentally tested by Han et al. (2017). The authors had monitored a gully in the Loess Plateau in China for 12 years, registering 115 erosive rainfall events. They concluded that the product of 30-minute intensity and total precipitation ( $P I_{30}$ ) was the key parameter to estimate total soil loss. Our results corroborate with this.

Furthermore, by applying the  $I_{30}$  in this study in order to estimate peak discharge and duration, it is implied that all the energy necessary to initiate and develop a gully channel comes from the most intense 30 minutes. Due to the limited number of gullies, it is not straightforward that the  $I_{30}$  could be the most representative index for any situation. Peak discharge and critical rainfall duration are often central variables in gully models (Foster and Lane, 1983; Hairsine and Rose, 1992; Sidorchuk, 1999; Gordon et al., 2007) and are related to erosion initiation parameters and thresholds, such as shear stress and stream power. This second factor has frequently been reported in literature as being more correlated with both laminar and linear erosion (Bennett and Wells, 2019). Figure 10a shows the performance of the tested intensities. Although the model using the 15-minute intensity presented smaller PBIAS and RMSE, the results indicated a large scatter around average.

Finally, The Foster and Lane Model also considers a fixed shear distribution, that is often unrealistic (Bonakdari et al., 2014) and fixed rectangular shape that, although frequently accurate for ephemeral gullies does not agree with field data and literature [Fig. 8; Starkel (2011)].

#### 4.1.2 Sidorchuk Model (SM)

The SM produced good results in this study, which were similar to those obtained by inserting a calibrated factor ( $\lambda$ ) in FLM. It is important to note that the original model used empirical correlations to determine width (Sidorchuk, 1999; Nachtergaele et al., 2002) and those were obtained for the Yamal basin. In the present study, we substituted this approximation for the width estimated by the FLM model, which permitted a more physical approach and increased the quality of the SM. The model was also capable to predict well the sidewall slope.

The model, however, showed a trend of overestimating smaller cross-sections (see Figure 7), mainly due to section geometry. When applied, the bottom width of the channel is considered to be the final width obtained by FLM. In larger sections, this hypothesis holds, once the discharge is large enough to carry all soil produced by sidewall erosion. In smaller sections, part of the soil is deposited and produces a V or U shaped cross-section (Starkel, 2011).

#### 4.1.3 Proposed Models

The FLM was further improved by the addition of the calibrated parameter  $\lambda$  (FLM- $\lambda$ ). This parameter is included to predict the effect of lateral discharges over wall erosion. Due to the significant improvement produced by its insertion, it could be understood that the original FLM fails to tackle this source of material (Blong and Veness, 1982; Crouch, 1987).

The FL-SM considers two sediment sources, channel bed and sidewall. Gullies are, however, complex systems with many sources and interactions. Headcut, sidewall erosion due to raindrops, flow jets and piping were not considered in our modelling approach. Processes of infiltration, subsurface flow and transport capacity were also neglected and should be properly addressed in future works. Nevertheless, the FL-SM assumptions managed to mimic well the field measurements, which implies that, at least in this study, the neglected processes are of lower relevance or were considered indirectly. For instance, sidewall erosion by raindrops can be considered insignificant over the wall failure process considered by Sidorchuk (1999). In addition, it is important to notice that, by selecting the 30-minute intensity, a less intense interval might be overlooked that produces erosive discharge, too, and can, therefore, explain the remaining processes.



One advantage of the FLM- $\lambda$  over the FL-SM is that the former require less data than the latter. The Sidorchuk model, and consequently the FL-SM require extra field work and laboratory analysis to assess root mass and plasticity index.

365 Despite the good results obtained from the modelling, the use of stochastic approaches (Sidorchuk, 2005) should improve the performance of the model and introduction of other sources of sediment. This is also relevant for generalisation and modelling of classical gullies. In the same way, the introduction of processes as armouring and energy losses as proposed by Hairsine and Rose (1992) can be interpreted as probabilistic terms.

370 Comparatively with other models, either physical or empirical (Hairsine and Rose, 1992; Woodward, 1999; Wells et al., 2013; Dabney et al., 2015), our proposed model (FL-SM) requires similar or less amount of data, little calibration (one parameter – the threshold) and is more versatile. Most models fail to account for multiple rainfall events (Foster and Lane, 1983; Woodward, 1999; Nachtergaele et al., 2002) and to consider multiple sources of sediment (Foster and Lane, 1983; Hairsine and Rose, 1992; Dabney et al., 2015). The FL-SM model ( $R^2 = 0.94$ ) presented better performance index than empirical models [e.g.  $R^2$ : 0.55 and 0.12 for Woodward (1999) and Wells et al. (2013) respectively] and physical models [e.g.  $R^2$ : 0.87 and 0.84 for Foster and Lane (1983) and Sidorchuk (1999) respectively]. This enhancing in the performance can be accounted for the  
375 more detailed modelling, considering wall failure and non-rectangular cross-section.

## 4.2 Data limitations

### 4.2.1 Topographic data

In terms of accuracy and agility, a topographic survey with UAV permits to measure sites within a few minutes. Conventional measurements, such as those with total station or profilometer, are more time consuming and do not grant better resolutions.  
380 The UAV accuracy, however, can be enhanced by performing flights in lower heights and more GCPs (Agüera-Vega et al., 2017; James et al., 2017), as well as by using high-end equipment, such as more robust UAVs and stabilizers. Total stations can also be used to improve the accuracy of ground control points (Mesas-Carrascosa et al., 2016). Given the scale of this study and the presented results of the models, the four-centimetre pixel represents a good resolution, since it combines good precision with affordable computational costs (Wang et al., 2016). The solution of UAV-based volume assessment is a good option for  
385 monitoring gully evolution (Stöcker et al., 2015), allowing frequent surveys, e.g., after every intense rainfall event.

However, trees and bushes obscure topographic measurements if too close to the gully channel and/or too dense in the catchment. Thus, UAV monitoring is more reliable for gully sites in non- or meagre-vegetated areas and meadows, which combines with the conditions of this study, except for gully 3 (G3), where it was impossible to accurately measure the total erosion volume due to relatively dense vegetation. It was, however, possible to select a large enough number of sections (eight)  
390 at G3 to assess the total erosion volume.

The topographic survey showed that all gullies had a significant portion of their watersheds occupied by the road, indicating a modification of the drainage system and change of the catchment boundaries – both causes of gully initiation foreseen by Ireland et al. (1939) – due to road construction, which promoted intense runoff and triggered gullies. Impacts of road construction on gully formation were also observed in Ethiopia (Nyssen et al., 2002) and the USA (Katz et al., 2014). Considering such

395 previous records in literature and the information collected with locals, the modelling considered 1958 as the start of gully erosion, coinciding with road construction.

### 4.3 Soil data

Though the three studied gullies are located in the same mesoscale basin, the Caatinga biome is known for its soil variability (Güntner and Bronstert, 2004) and soil properties do differ among the gullies. However, only small changes of texture were  
400 observed in different depths, allowing an analysis based on average properties. Nevertheless, for deeper and/or more variable soils, the discretization of soil properties, and therefore parameters such as rill erodibility ( $K_r$ ) and critical shear stress ( $\tau_c$ ) can easily be taken into account. The good performance of the final model (FL-SM) also indicates that the WEPP equations for critical shear stress and rill erodibility (Eq. 1 and 2) can be used for the soils of the region. These equations were obtained via regression curves from data collected on 34 plot areas in the USA with a wide range of textures, slopes, land use and  
405 land cover. The areas from the WEPP model possess different geological and climatic conditions from the soils in the Brazilian Semiarid Region; this is why local studies should be carried out, since empirical equations frequently have strong local character (Ghorbani-Dashtaki et al., 2016; Dionizio and Costa, 2019).

### 4.4 Rainfall data

This study shows that sub-daily information of rainfall is of crucial importance for gully modelling. In this study, we used  
410 correlation curves based on long-term time series of a similar catchment in the region. However, such analysis might introduce an averaged and monotonic behaviour for the intensities, as presented in Figure 4, and is, therefore, unrealistic. Stochastic models should be tested to estimate sub-daily information from daily rainfall. The estimation of discharge from rainfall can also be improved by considering water content in the soil and modelling its evolution over the studied period using water balance models.

## 415 5 Conclusions

In this study, efforts were concentrated on understanding how the cross-section of small permanent gullies (with no groundwater contributions) evolve. It was possible to identify two main mechanisms: the first is bed erosion, governed by shear stress at the bottom of the channel. The second is the sidewall erosion due to gravitational processes and lateral flow. To successfully model both components, two models were coupled – those by Foster and Lane (1983) and Sidorchuk (1999). The two mechanisms,  
420 however, do not happen simultaneously in all sections, they depend on the process scale and are ruled by a threshold of eroded cross-section area. To model the gullies in a region without local data of sub-daily rainfall, correlation curves were used to estimate rain intensity from total daily precipitation. For the purpose of modelling peak discharges, the intensity that showed the best results was the 30-minute one ( $I_{30}$ ).

Gully is an erosion related to many processes and it is scale dependent. The attempt of proposing a generalist model for  
425 gullies should also consider these different scales and mechanisms involved in different stages of the gully development.

Catchment shape and lateral flow have a central role on gully erosion and their influence should be further investigated. Infrastructure constructions, as roads, change conditions for gully initiation and was the trigger for the studied gullies.

430 The proposed final model (FL-SM; standing for Foster & Lane and Sidorchuk Model) presented a performance that varied from acceptable to very good, depending on the criteria. This model managed to estimate total erosion in a small permanent gully for a total period of six decades. Despite the good results of FL-SM, more efforts should be undertaken to tackle other sources of gully sediments, such as headcut and piping.

Nonetheless, much efforts are required to fully model gully erosion, such as include the multiple other sources, such as headcut, pipping, channel shear stress and flow jets. also,, stochastic modelling should be implemented, in order to tackle inherent uncertainties of many sediment sources and lack of data.

435 *Code and data availability.* Code and data available in the link: <https://github.com/PedroAlencarTUB/GullyModel-FLSM>

*Author contributions.* Alencar worked on fieldwork, programming, laboratory analysis. Teixeira carried image acquisition and processing. de Araújo acted as supervisor of the work and in its conceptualization. Alencar prepared the text with contributions of all authors.

*Competing interests.* The authors declare that they have no conflict of interest.

This work is part of the PhD work of **Pedro Alencar** and will be used in his dissertation.

440 *Disclaimer.*

*Acknowledgements.* This study was partly financed by the *Coordenação de Aperfeiçoamento de Pessoal de Nível Superior - Brasil (CAPES)* - Finance Code 001 and by the *Edital Universal CNPq* - number 407999/2016-7. Pedro Alencar is funded by the DAAD. Many thanks to Prof. Eva Paton for the support and advising at the Technische Universität Berlin.

## References

- 445 Agüera-Vega, F., Carvajal-Ramírez, F., and Martínez-Carricondo, P.: Assessment of photogrammetric mapping accuracy based on variation ground control points number using unmanned aerial vehicle, *Measurement*, 98, 221–227, 2017.
- Alberts, E. E., Nearing, M. A., Weltz, M. A., Risse, L. M., Pierson, F. B., Zhang, X. C., Lafren, J. M., and Simanton, J. R.: Soil Component, Tech. Rep. July, USDA, 1995.
- Arabameri, A., Cerda, A., and Tiefenbacher, J. P.: Spatial Pattern Analysis and Prediction of Gully Erosion Using Novel Hybrid Model of Entropy-Weight of Evidence, *Water*, 11, 1129, 2019.
- 450 Azareh, A., Rahmati, O., Rafiei-Sardooi, E., Sankey, J. B., Lee, S., Shahabi, H., and Ahmad, B. B.: Modelling gully-erosion susceptibility in a semi-arid region, Iran: Investigation of applicability of certainty factor and maximum entropy models, *Science of the Total Environment*, <https://doi.org/10.1016/j.scitotenv.2018.11.235>, 2019.
- Bennett, S. J. and Wells, R. R.: Gully erosion processes, disciplinary fragmentation, and technological innovation, *Earth Surface Processes and Landforms*, 44, 46–53, <https://doi.org/10.1002/esp.4522>, 2019.
- 455 Bernard, J., Lemunyon, J., Merkel, B., Theurer, F., Widman, N., Bingner, R., Dabney, S., Langendoen, E., Wells, R., and Wilson, G.: Ephemeral Gully Erosion — A National Resource Concern., U.S. Department of Agriculture. NSL Technical Research Report No. 69, p. 67 pp, 2010.
- Bingner, R. L., Wells, R. R., Momm, H. G., Rigby, J. R., and Theurer, F. D.: Ephemeral gully channel width and erosion simulation technology, *Natural Hazards*, 80, 1949–1966, <https://doi.org/10.1007/s11069-015-2053-7>, 2016.
- 460 Blong, R. J. and Veness, J. A.: The Role of Sidewall Processes in Gully Development, *Earth Surface Processes and Landforms*, 7, 381–385, 1982.
- Bonakdari, H., Sheikh, Z., and Tooshmalani, M.: Comparison between Shannon and Tsallis entropies for prediction of shear stress distribution in open channels, *Stochastic Environmental Research and Risk Assessment*, 29, 1–11, <https://doi.org/10.1007/s00477-014-0959-3>, 2014.
- 465 Borrelli, P., Robinson, D. A., Fleischer, L. R., Lugato, E., Ballabio, C., Alewell, C., Meusburger, K., Modugno, S., Schütt, B., Ferro, V., Bagarello, V., Oost, K. V., Montanarella, L., and Panagos, P.: An assessment of the global impact of 21st century land use change on soil erosion, *Nature Communications*, 8, <https://doi.org/10.1038/s41467-017-02142-7>, 2017.
- Castillo, C. and Gómez, J. A.: A century of gully erosion research: Urgency, complexity and study approaches, *Earth-Science Reviews*, 160, 300–319, <https://doi.org/10.1016/j.earscirev.2016.07.009>, 2016.
- 470 Chow, V. T.: *Open-channel hydraulics*, in: *Open-channel hydraulics*, McGraw-Hill, 1959.
- Coelho, C., Heim, B., Foerster, S., Brosinsky, A., and de Araújo, J. C.: In situ and satellite observation of CDOM and chlorophyll-a dynamics in small water surface reservoirs in the brazilian semiarid region, *Water (Switzerland)*, 9, <https://doi.org/10.3390/w9120913>, 2017.
- Crouch, R. J.: The relationship of gully sidewall shape to sediment production, *Australian Journal of Soil Research*, 25, 531–539, 1987.
- da Silva, A. J. P. and Rios, M. L.: Alerta de desertificação no médio curso do Rio Salitre, afluente do Rio São Francisco, Tech. rep., IFBA, 475 Senhor do Bonfim, Bahia, 2018.
- Dabney, S. M., Vieira, D. A. N., Yoder, D. C., Langendoen, E. J., Wells, R. R., and Ursic, M. E.: Spatially Distributed Sheet, Rill, and Ephemeral Gully Erosion, *Journal of Hydrologic Engineering*, 20, C4014 009, 2015.
- de Araújo, J. C. and Piedra, J. I. G.: Comparative hydrology: analysis of a semiarid and a humid tropical watershed, *Hydrological Process*, 23, 1169–1178, <https://doi.org/10.1002/hyp>, 2009.

- 480 de Araújo, J. C., Güntner, A., and Bronstert, A.: Loss of reservoir volume by sediment deposition and its impact on water availability in semiarid Brazil / Perte de volume de stockage en réservoirs par sédimentation et impact sur la disponibilité en eau au Brésil semi-aride  
Loss of reservoir volume by se, *Hydrological Sciences Journal*, 51, 157–170, <https://doi.org/10.1623/hysj.51.1.157>, 2006.
- Dionizio, E. A. and Costa, M. H.: Influence of Land Use and Land Cover on Hydraulic and Physical Soil Properties at the Cerrado Agricultural Frontier, *Agriculture*, 9, 14, <https://doi.org/10.3390/agriculture9010024>, 2019.
- 485 dos Santos, J. C. N., de Andrade, E. M., Guerreiro, M. J. S., Medeiros, P. H. A., de Queiroz Palácio, H. A., and de Araújo Neto, J. R.: Effect of dry spells and soil cracking on runoff generation in a semiarid micro watershed under land use change, *Journal of Hydrology*, 541, 1–10, <https://doi.org/10.1016/j.jhydrol.2016.08.016>, 2016.
- Figueiredo, J. V., Araújo, J. C., Medeiros, P. H. A., and Costa, A. C.: Runoff initiation in a preserved semiarid Caatinga small watershed, Northeastern Brazil, *Hydrological Processes*, 30, 2390–2400, <https://doi.org/10.1002/hyp.10801>, 2016.
- 490 Foster, G. R. and Lane, L. J.: Erosion by concentrated flow in farm fields, in: D.B. Simons Symposium on Erosion and Sedimentation, p. 21, 1983.
- Gaiser, T., Krol, M., Frischkom, H., and de Araujo, J. C., eds.: *Global Change and Regional Impacts*, Springer-Verlag, Berlin, [https://doi.org/10.1007/978-3-642-55659-3\\_9](https://doi.org/10.1007/978-3-642-55659-3_9), 2003.
- Ghorbani-Dashtaki, S., Homae, M., and Loiskandl, W.: Towards using pedotransfer functions for estimating infiltration parameters, *Hydro-*  
495 *logical Sciences Journal*, 61, 1477–1488, <https://doi.org/10.1080/02626667.2015.1031763>, 2016.
- Gordon, L. M., Bennett, S. J., Bingner, R. L., Theurer, F. D., and Alonso, C. V.: Simulating Ephemeral Gully Erosion in AnnAGNPS, *Transactions of the ASAE*, 50, 857–866, 2007.
- Güntner, A. and Bronstert, A.: Representation of landscape variability and lateral redistribution processes for large-scale hydrological modelling in semi-arid areas, *Journal of Hydrology*, 297, 136–161, <https://doi.org/10.1016/j.jhydrol.2004.04.008>, 2004.
- 500 Hairsine, P. B. and Rose, C. W.: Modeling water erosion due to overland flow using physical principles: 2. Rill flow, *Water Resources Research*, 28, 245–250, <https://doi.org/10.1029/91WR02381>, 1992.
- Han, Y., li Zheng, F., and meng Xu, X.: Effects of rainfall regime and its character indices on soil loss at loessial hillslope with ephemeral gully, *Journal of Mountain Science*, 14, 527–538, <https://doi.org/10.1007/s11629-016-3934-2>, 2017.
- Hunke, P., Mueller, E. N., Schröder, B., and Zeilhofer, P.: The Brazilian Cerrado: Assessment of water and soil degradation in catchments  
505 under intensive agricultural use, *Ecology*, 8, 1154–1180, <https://doi.org/10.1002/eco.1573>, 2015.
- Ireland, H., Sharpe, C. F. S., and Eargle, D. H.: *Principles of Gully Erosion in the Piedmont of South Carolina*, Tech. rep., USDA, Washington, 1939.
- James, M. R., Robson, S., Oleire-Oltmanns, S., and Niethammer, U.: Geomorphology Optimising UAV topographic surveys processed with structure-from-motion : Ground control quality , quantity and bundle adjustment, *Geomorphology*, 280, 51–66, 2017.
- 510 Katz, H. A., Daniels, J. M., and Ryan, S.: Slope-area thresholds of road-induced gully erosion and consequent hillslope-channel interactions, *Earth Surface Processes and Landforms*, 39, 285–295, <https://doi.org/10.1002/esp.3443>, 2014.
- Liu, X. L., Tang, C., Ni, H. Y., and Zhao, Y.: Geomorphologic analysis and a physico-dynamic characteristics of Zhatai-Gully debris flows in SW China, *Journal of Mountain Science*, 13, 137–145, 2016.
- Maetens, W., Vanmaercke, M., Poesen, J., Jankauskas, B., Jankauskiene, G., and Ionita, I.: Effects of land use on annual runoff  
515 and soil loss in Europe and the Mediterranean: A meta-analysis of plot data, *Progress in Physical Geography*, 36, 599–653, <https://doi.org/10.1177/0309133312451303>, 2012.

- Medeiros, P. H. A. and Araújo, J. C. D.: Temporal variability of rainfall in a semiarid environment in Brazil and its effect on sediment transport processes, *Journal of Soils and Sediments*, pp. 1216–1223, <https://doi.org/10.1007/s11368-013-0809-9>, 2014.
- 520 Mendes, F. J.: Uma Proposta de Reclassificação das Regiões Pluviometricamente Homogêneas do Estado do Ceará, Dissertação, Universidade Estadual do Ceará, 2010.
- Mesas-Carrascosa, F. J., García, M. D. N., De Larriva, J. E. M., and García-Ferrer, A.: An analysis of the influence of flight parameters in the generation of unmanned aerial vehicle (UAV) orthomosaics to survey archaeological areas, *Sensors (Switzerland)*, 16, 2016.
- Montgomery, D. and Dietrich, W.: Channel Initiation and Problem of Landscape Scale, *Science*, 255, 826–830, 1992.
- Moriasi, D. N., Arnold, J. G., Van Liew, M. W., Bingner, R. L., Harmel, R. D., and Veith, T. L.: Model Evaluation Guidelines for Systematic Quantification of Accuracy in Watershed Simulations, *Transactions of the ASABE*, 50, 885–900, 2007.
- 525 Mutti, P. R., Lúcio, P. S., Dubreuil, V., and Bezerra, B. G.: NDVI time series stochastic models for the forecast of vegetation dynamics over desertification hotspots, *International Journal of Remote Sensing*, 41, 2759–2788, <https://doi.org/10.1080/01431161.2019.1697008>, 2020.
- Nachtergaele, J., Poesen, J., Sidorchuk, A., and Torri, D.: Prediction of concentrated flow width in ephemeral gully channels, *Hydrological Processes*, 16, 1935–1953, <https://doi.org/10.1002/hyp.392>, 2002.
- 530 Nkonya, E., Anderson, W., Kato, E., Koo, J., Mirzabaev, A., von Braun, J., and Meyer, S.: Global Cost of Land Degradation, in: *Economics of Land Degradation and Improvement - A Global Assessment for Sustainable Development*, edited by Nkonya, E., Mirzabaev, A., and von Braun, J., chap. 6, pp. 117–165, Springer Open, Cham, <https://doi.org/10.1007/978-3-319-19168-3>, 2016.
- Nyssen, J., Poesen, J., Moeyersons, J., Luyten, E., Veyret-Picot, M., Deckers, J., Haile, M., and Govers, G.: Impact of Road Building on Gully Erosion Risk: a Case of Study from the Northern Ethiopian Highlands, *Earth Surface Processes and Landforms*, 27, 1267–1283, 535 2002.
- Panagos, P., Ballabio, C., Meusburger, K., Spinoni, J., Alewell, C., and Borrelli, P.: Towards estimates of future rainfall erosivity in Europe based on REDES and WorldClim datasets, *Journal of Hydrology*, 548, 251–262, <https://doi.org/10.1016/j.jhydrol.2017.03.006>, 2017.
- Paton, E. N., Smetanová, A., Krueger, T., and Parsons, A.: Perspectives and ambitions of interdisciplinary connectivity researchers, *Hydrology and Earth System Sciences*, 23, 537–548, <https://doi.org/10.5194/hess-23-537-2019>, 2019.
- 540 Pinheiro, E. A. R., Costa, C. A. G., and Araújo, J. C. D.: Effective root depth of the Caatinga biome, *Arid Environments*, 89, 4, 2013.
- Pinheiro, E. A. R., Metselaar, K., de Jong van Lier, Q., and de Araújo, J. C.: Importance of soil-water to the Caatinga biome, Brazil, *Ecohydrology*, 9, 1313–1327, <https://doi.org/10.1002/eco.1728>, 2016.
- Poesen, J.: Soil erosion in the Anthropocene: Research needs, *Earth Surface Processes and Landforms*, 43, 64–84, <https://doi.org/10.1002/esp.4250>, 2018.
- 545 Poesen, J., Vanwalleghem, T., De Vente, J., Knapen, A., Verstraeten, G., and Martínez-Casasnovas, J. A.: Gully Erosion in Europe, in: *Soil Erosion in Europe*, chap. 39, pp. 515–536, John Wiley & Sons Ltd, <https://doi.org/10.1002/0470859202.ch39>, 2006.
- Ritter, A. and Muñoz-Carpena, R.: Performance evaluation of hydrological models : Statistical significance for reducing subjectivity in goodness-of-fit assessments, *Journal of Hydrology*, 480, 33–45, <https://doi.org/10.1016/j.jhydrol.2012.12.004>, 2013.
- Sartori, M., Philippidis, G., Ferrari, E., Borrelli, P., Lugato, E., Montanarella, L., and Panagos, P.: A linkage between the biophysical and the economic: Assessing the global market impacts of soil erosion, *Land Use Policy*, 86, 299–312, 2019.
- 550 Sassolas-Serrayet, T., Cattin, R., and Ferry, M.: The shape of watersheds, *Nature Communications*, 9, 1–8, 2018.
- Sena, A., Barcellos, C., Freitas, C., and Corvalan, C.: Managing the health impacts of drought in Brazil, *International Journal of Environmental Research and Public Health*, 11, 10737–10751, <https://doi.org/10.3390/ijerph111010737>, 2014.
- Sidorchuk, A.: Dynamic and static models of gully erosion, *Catena*, 37, 401–414, [https://doi.org/10.1016/S0341-8162\(99\)00029-6](https://doi.org/10.1016/S0341-8162(99)00029-6), 1999.

- 555 Sidorchuk, A.: Stochastic components in the gully erosion modelling, *Catena*, 63, 299–317, 2005.
- Silva, E., Gorayeb, A., and de Araújo, J.: Atlas socioambiental do Assentamento 25 de Maio-Madalena-Ceará, Fortaleza: Ed. Expressão Gráfica, 2015.
- Starkel, L.: Paradoxes in the development of gullies, *Landform Analysis*, 17, 11–13, 2011.
- Stöcker, C., Eltner, A., and Karrasch, P.: Measuring gullies by synergetic application of UAV and close range photogrammetry - A case study from Andalusia, Spain, *Catena*, 132, 1–11, <https://doi.org/10.1016/j.catena.2015.04.004>, 2015.
- 560 Thompson, J. R.: Quantitative Effect of Watershed Variables on Rate of Gully-Head Advancement, *Transactions of the ASAE*, 7, 0054–0055, 1964.
- Torri, D. and Poesen, J.: A review of topographic threshold conditions for gully head development in different environments, *Earth Science Reviews*, 130, 73–85, <https://doi.org/10.1016/j.earscirev.2013.12.006>, 2014.
- 565 Valentin, C., Poesen, J., and Li, Y.: Gully erosion: Impacts, factors and control, *Catena*, 63, 132–153, 2005.
- van Schaik, N. L., Bronstert, A., de Jong, S. M., Jetten, V. G., van Dam, J. C., Ritsema, C. J., and Schnabel, S.: Process-based modelling of a headwater catchment in a semi-arid area: The influence of macropore flow, *Hydrological Processes*, 28, 5805–5816, 2014.
- Vandaele, K., Poesen, J. A. W., Govers, G., and van Wesemael, B.: Geomorphic threshold conditions for ephemeral gully incision, *Geomorphology*, 16, 161–173, 1996.
- 570 Vannoppen, W., De Baets, S., Keeble, J., Dong, Y., and Poesen, J.: How do root and soil characteristics affect the erosion-reducing potential of plant species?, *Ecological Engineering*, 109, 186–195, <https://doi.org/10.1016/j.ecoleng.2017.08.001>, 2017.
- Vanwalleghem, T., Poesen, J., Nachtergaele, J., Deckers, J., and Eeckhaut, M. V. D.: Reconstructing rainfall and land-use conditions leading to the development of old gullies, *The Holocene*, 15, 378–386, 2005.
- Verstraeten, G., Bazzoffi, P., Lajczak, A., Rădoane, M., Rey, F., Poesen, J., and De Vente, J.: Reservoir and Pond Sedimentation in Europe, *Soil Erosion in Europe*, pp. 757–774, <https://doi.org/10.1002/0470859202.ch54>, 2006.
- 575 Wang, R., Zhang, S., Pu, L., Yang, J., Yang, C., Chen, J., Guan, C., Wang, Q., Chen, D., Fu, B., and Sang, X.: Gully Erosion Mapping and Monitoring at Multiple Scales Based on Multi-Source Remote Sensing Data of the Sancha River Catchment, Northeast China, *ISPRS International Journal of Geo-Information*, 5, 200, <https://doi.org/10.3390/ijgi5110200>, 2016.
- Wei, R., Zeng, Q., Davies, T., Yuan, G., Wang, K., Xue, X., and Yin, Q.: Geohazard cascade and mechanism of large debris flows in Tianmo gully, SE Tibetan Plateau and implications to hazard monitoring, *Engineering Geology*, 233, 172–182, 2018.
- 580 Wells, R. R., Momm, H. G., Rigby, J. R., Bennett, S. J., Bingner, R. L., and Dabney, S. M.: An empirical investigation of gully widening rates in upland concentrated flows, *Catena*, 101, 114–121, <https://doi.org/10.1016/j.catena.2012.10.004>, 2013.
- Wischmeier, W. H. and Smith, D. D.: Predicting rainfall erosion losses - a guide to conservation planning, Tech. rep., USDA, Hyattsville, 1978.
- 585 Woodward, D. E.: Method to predict cropland ephemeral gully erosion, *Catena*, 37, 393–399, 1999.
- Yibeltal, M., Tsunekawa, A., Haregeweyn, N., Adgo, E., Meshesha, D. T., Aklog, D., Masunaga, T., Tsubo, M., Billi, P., Vanmaercke, M., Ebabu, K., Dessie, M., Sultan, D., and Liyew, M.: Analysis of long-term gully dynamics in different agro-ecology settings, *Catena*, 179, 160–174, <https://doi.org/10.1016/j.catena.2019.04.013>, 2019.
- Zhang, S., Foerster, S., Medeiros, P., de Araújo, J. C., and Waske, B.: Effective water surface mapping in macrophyte-covered reservoirs in NE Brazil based on TerraSAR-X time series, *International Journal of Applied Earth Observation and Geoinformation*, 69, 41–55, <https://doi.org/10.1016/j.jag.2018.02.014>, 2018.
- 590



Zweig, R., Filin, S., Avni, Y., Sagy, A., and Mushkin, A.: Land degradation and gully development in arid environments deduced by mezzo- and micro-scale 3-D quantification – The Negev Highlands as a case study, *Journal of Arid Environments*, 153, 52–65, <https://doi.org/10.1016/j.jaridenv.2017.12.006>, 2018.